



UNIVERSITI PUTRA MALAYSIA

***FABRICATION OF BARIUM HEXAFERRITE NANOCOMPOSITE AND
HYBRID MULTIWALLED CARBON NANOTUBES/BARIUM
HEXAFERRITE AS MICROWAVE ABSORBING MATERIAL***

NURSHAHIERA BINTI ROSDI

ITMA 2022 10



UPM
UNIVERSITI PUTRA MALAYSIA
BERILMU BERBAKTI

**FABRICATION OF BARIUM HEXAFERRITE NANOCOMPOSITE AND
HYBRID MULTIWALLED CARBON NANOTUBES/BARIUM HEXAFERRITE
AS MICROWAVE ABSORBING MATERIAL**

By

NURSHAHIERA BINTI ROSDI

**Thesis Submitted to the School of Graduate Studies, Universiti Putra
Malaysia, in Fulfilment of the Requirements for the Degree of Master of
Science**

February 2022

All material contained within the thesis, including without limitation text, logos, icons, photographs and all other artwork, is copyright material of Universiti Putra Malaysia unless otherwise stated. Use may be made of any material contained within the thesis for non-commercial purposes from the copyright holder. Commercial use of material may only be made with the express, prior, written permission of Universiti Putra Malaysia.

Copyright © Universiti Putra Malaysia



Abstract of thesis presented to the Senate of Universiti Putra Malaysia in fulfillment of the requirement for the degree of Master of Science

FABRICATION OF BARIUM HEXAFERRITE NANOCOMPOSITE AND HYBRID MULTIWALLED CARBON NANOTUBES/BARIUM HEXAFERRITE AS MICROWAVE ABSORBING MATERIAL

By

NURSHAHIERA BINTI ROSDI

February 2022

Chair : Assoc. Prof. Raba'ah Syahidah Azis, PhD
Institute : Nanoscience and Nanotechnology

This research work studied the synthesis of barium hexaferrite (BHF) in detail, focusing on their microstructure, magnetic, and microwave properties. As the raw material for this project, the iron (III) oxide, Fe_2O_3 , is utilized and processed from mill scale waste. The iron (III) oxide, Fe_2O_3 , then mixed with barium carbonate (BaCO_3) to synthesize the barium hexaferrite ($\text{BaFe}_{12}\text{O}_{19}$, BHF) by employing the high-energy ball milling (HEBM) technique for 3 hours, a single milling (SM) process. The BHF-SM samples were then sintered from 800 °C to 1400 °C with an increment of 100 °C. The sintered BHF-SM samples was again employing by HEBM technique for 3 hours, a double milling (DM) process. The samples after double milling process namely as BHF-DM. The hybrid multiwalled carbon nanotubes (MWCNTs)/BHF has been introduced in this research. The structural, microstructure and magnetic properties of the prepared samples were examined using an X-ray diffractometer (XRD), vibrating sample magnetometer (VSM), and field emission scanning electron (FESEM), respectively. Vector network analyzer (VNA) has been used for measuring Reflection Loss (RL), complex permeability (μ_r) and complex permittivity (ϵ_r) in frequency ranges at X and Ku band (8-18 GHz). The RL for BHF-SM and BHF-DM nanocomposites are samples sintered at 1400 °C, shows the maximum RL with -13.71 dB is at the frequency of 9.96 GHz with a bandwidth of 0.24 GHz at a thickness of 3 mm and -35.57 dB at 12.33 GHz with a bandwidth of 1.2 GHz at a thickness of 2 mm, respectively. The hybrid MWCNTs/BHF-SM sample with 10 wt% filler content could enhance the RL values up to -43.99 dB at a frequency of 12.96 GHz with bandwidth of 2.56 GHz at a thickness of 2 mm. As for hybrid MWCNTs/BHF-DM sample, the RL is approximately -32.49 dB at 12.9 GHz with a bandwidth of 2.31 GHz at a thickness 2 mm. Generally, it was found that hybrid

is a most highly potential candidate as ideal MAMs due to high microwave attenuation performances, enhanced the RL of and wide bandwidth.



Abstrak tesis yang dikemukakan kepada Senat Universiti Putra Malaysia
sebagai memenuhi keperluan untuk Ijazah Master Sains

**FABRIKASI BARIUM HEKSAFERIT NANOKOMPOSIT DAN HIBRID
MULTIDINDING KARBON TIUB NANO/BARIUM HEKSAFERIT SEBAGAI
BAHAN PENYERAP GELOMBANG MIKRO**

Oleh

NURSHAHIERA BINTI ROSDI

Februari 2022

Pengerusi : Prof. Madya. Raba'ah Syahidah Azis, PhD
Institut : Nanosains dan Nanoteknologi

Kerja penyelidikan ini mengkaji sintesis barium heksaferit (BHF) secara terperinci, dengan memfokuskan pada struktur mikro, magnetik, dan sifat gelombang mikro. Sebagai bahan mentah untuk projek ini, besi (III) oksida, Fe_2O_3 , telah digunakan dan diproses daripada buangan sisik besi. Besi (III) oksida, Fe_2O_3 , kemudian dicampur dengan barium karbonat (BaCO_3) untuk mensintesis barium heksaferit ($\text{BaFe}_{12}\text{O}_{19}$, BHF) dengan menggunakan teknik pengisar bebola kuasa tinggi (HEBM) selama 3 jam, bagi proses penggilingan tunggal (SM). Sampel BHF-SM kemudian disinter dari $800\text{ }^\circ\text{C}$ hingga $1400\text{ }^\circ\text{C}$ dengan kenaikan $100\text{ }^\circ\text{C}$. BHF-SM yang disinter itu sekali lagi menggunakan teknik pengisar bebola kuasa tinggi (HEBM) selama 3 jam, bagi proses penggilingan ganda (DM). Sampel-sampel selepas proses penggilingan ganda dinamakan sebagai BHF-DM. Hibrid karbon tiub nano multidinding (MWCNTs)/BHF telah diperkenalkan dalam penyelidikan ini. Sifat struktur, mikro dan magnet bagi sampel yang disediakan telah dilaksanakan melalui pembelauan sinar-X (XRD), penggetar sampel magnetometer (VSM), dan pengimbas mikroskop elektron (FESEM). Penganalisis rangkaian vektor (VNA) telah digunakan untuk mengukur kehilangan pantulan (RL), kebolehtelapan kompleks (μ_r) dan ketelusan kompleks (ϵ_r) dalam julat frekuensi pada jalur X dan Ku (8-18 GHz). Kehilangan pantulan untuk sampel BHF-SM dan BHF-DM nanokomposit yang disinter pada $1400\text{ }^\circ\text{C}$, menunjukkan kehilangan pantulan maksimum dengan -13.71 dB pada frekuensi 9.96 GHz dengan lebar julat 0.24 GHz pada ketebalan 3 mm dan -35.57 dB pada 12.33 GHz dengan lebar julat 1.2 GHz pada ketebalan 2 mm, masing-masing. Sampel hibrid MWCNTs/BHF-SM dengan kandungan berat pengisi 10 wt% boleh meningkatkan nilai kehilangan pantulan sehingga -43.99 dB pada frekuensi 12.96 GHz dengan lebar julat 2.56 GHz pada ketebalan 2 mm. Bagi sampel hibrid MWCNTs/BHF-DM, kehilangan pantulan adalah lebih kurang -32.49 dB pada 12.9 GHz dengan

lebar julat 2.31 GHz pada ketebalan 2 mm. Secara amnya, didapati bahawa hibrid ialah bahan yang paling berpotensi sebagai bahan penyerap gelombang yang ideal disebabkan oleh prestasi pengecilan gelombang mikro yang tinggi, dapat meningkatkan nilai kehilangan pantulannya dengan lebar julat yang lebih besar.



ACKNOWLEDGEMENTS

In the name of Allah, the most gracious and the most merciful

My sincere gratitude goes to thr Creator of the heavens and earths and what's in between; the Almighty Allah, glorified be He, then to His prophet, Nabi Muhammad S.A.W.

I would like to express my deepest sense of gratitude to my supervisor, Associate Prof. Dr. Raba'ah Syahidah Azis for his supervision and constant support throughout this valuable journey. I am really grateful to have a very positive and understanding supervisor and his patience to handle my shortcoming and continuous questions, from which I have learned a lot. I really appreciate her as a really kind supervisor and take him as an admirable example for my future academic career. I wish to express my gratitude to my co-supervisor Dr. Ismayadi Ismail and Dr. Nurhidayat Mokhtar for their wisely suggestion, guidance and help throughout the project.

I also acknowledge fruitful discussions from the research group members, such as Dr. Idza Ibrahim, Muhammad Misbah Muhamad Zulkimi, Farah Nabilah Shaafie, Dr. Hapishah Abdullah, Dr. Muhammad Syazwan Mustafa, Syazana Sulaiman, Nur Shamimi Akmal Azany and Siti Aisah Harun. I am also grateful to Mr. Mohd Kadri Masaud, Mr. Md Ali Rani, and Mrs. Sarinawani Abdul Ghani for their guidance on using the instruments in the laboratory.

My deepest appreciation goes to Universiti Putra Malaysia under Graduate Research Fellowship (GRF).

Last but not least, a very important person which are my parents Rosdi Bin Mohd Nor and Selamah Binti Salleh. Thank you so much for their support and sacrifice throughout my study. This dissertation is simply impossible without you. I love you so much. Special thanks and deep love to my siblings Rohaiza Rosdi, Mohd Mustafa Rosdi and Norazzwa Rosdi. Thank you all for always being my side throughout my good times and in those more critical moments. I love all of you.

This thesis was submitted to the Senate of Universiti Putra Malaysia and has been accepted as fulfilment of the requirement for the degree of Master of Science. The members of the Supervisory Committee were as follows:

Raba'ah Syahidah binti Azis, PhD

Associate Professor
Faculty of Science
Universiti Putra Malaysia
(Chairman)

Nurhidayaty binti Mokhtar, PhD

Senior Lecturer
Faculty of Science
Universiti Putra Malaysia
(Member)

Ismayadi bin Ismail, PhD

Senior Lecturer
Institute of Nanoscience and Nanotechnology
Universiti Putra Malaysia
(Member)

ZALILAH MOHD SHARIFF, PhD

Professor and Dean
School of Graduate Studies
Universiti Putra Malaysia

Date: 13 October 2022

Declaration by Graduate Student

I hereby confirm that:

- this thesis is my original work;
- quotations, illustrations and citations have been duly referenced;
- this thesis has not been submitted previously or concurrently for any other degree at any institutions;
- intellectual property from the thesis and the copyright of the thesis are fully-owned by Universiti Putra Malaysia, as stipulated in the Universiti Putra Malaysia (Research) Rules 2012;
- written permission must be obtained from the supervisor and the office of the Deputy Vice-Chancellor (Research and innovation) before the thesis is published in any written, printed or electronic form (including books, journals, modules, proceedings, popular writings, seminar papers, manuscripts, posters, reports, lecture notes, learning modules or any other materials) as stated in the Universiti Putra Malaysia (Research) Rules 2012;
- there is no plagiarism or data falsification/fabrication in the thesis, and scholarly integrity is upheld in accordance with the Universiti Putra Malaysia (Graduate Studies) Rules 2003 (Revision 2015-2016) and the Universiti Putra Malaysia (Research) Rules 2012. The thesis has undergone plagiarism detection software

Signature: _____ Date: _____

Name and Matric No.: Nurshahiera binti Rosdi

Declaration by Members of Supervisory Committee

This is to confirm that:

- the research and the writing of this thesis were done under our supervision;
- supervisory responsibilities as stated in the Universiti Putra Malaysia (Graduate Studies) Rules 2003 (Revision 2015-2016) are adhered to.

Signature: _____
Name of Chairman
of Supervisory Committee: Assoc. Prof. Raba'ah Syahidah
Azis

Signature: _____
Name of Member of
Supervisory Committee: Dr. Nurhidayat Mokhtar

Signature: _____
Name of Member of
Supervisory Committee: Dr. Ismayadi Ismail

TABLE OF CONTENTS

	Page
ABSTRACT	i
ABSTRAK	iii
ACKNOWLEDGEMENTS	v
APPROVAL	vi
DECLARATION	viii
LIST OF TABLES	xiii
LIST OF FIGURES	xv
LIST OF ABBREVIATIONS	xxvi
CHAPTER	
1 INTRODUCTION	
1.1 Background of the study	1
1.2 A potential of raw material waste mill scale	3
1.3 Potential Multiwalled Carbon Nanotubes (MWCNTs) as microwave absorbing materials	4
1.4 Problem Statement	4
1.5 Objectives	5
1.5.1 Main research project objective	5
1.5.2 Work-phase Objectives	5
1.6 Limitations of study	6
1.7 Outlines of the thesis	6
2 LITERATURE REVIEW	
2.1 Introduction	7
2.2 Selection of material	7
2.2.1 Ferrites	7
2.2.2 Hard Ferrite Magnetic	8
2.2.3 M-Type Ferrites	9
2.2.4 Application of Hard Ferrites	9
2.3 Processing technique of Iron oxide using mill scale waste	10
2.4 Barium Hexaferrite (BHF) material as Microwave Absorbing Materials	11
2.5 Synthesis method of Barium Hexaferrite (BHF) material as microwave absorbing materials	15
2.5.1 High Energy Ball Milling	15
2.6 Influence of multiwalled carbon nanotubes (MWCNTs) material based for microwave absorption characteristics	19
2.7 New approach from this research work	22
3 THEORY	
3.1 Introduction	23
3.2 Hexagonal ferrites	23
3.3 M-type hexaferrite	24

3.4	Crystal structure of M-type hexaferrite	24
3.5	Magnetic properties of hexaferrite	26
3.6	Theory on Electromagnetic Wave Absorption	29
3.7	Reflection Loss in Microwave Absorbing Materials	30
3.8	Microwave properties for absorbing materials	33
3.9	Influencing Factors of Microwave Absorption	34
3.9.1	Intrinsic Factors	34
3.9.2	Extrinsic Factors	40
4	METHODOLOGY	
4.1	Introduction	42
4.2	Research design	42
4.3	Preparation of hematite, Fe ₂ O ₃	47
4.3.1	Selection of mill scales waste	47
4.3.2	Weighing of mill scale waste	47
4.3.3	Grinding of mill scale waste (24 hours)	47
4.3.4	Magnetic Separation Technique (MST)	48
4.3.5	Curie Temperature Separation Technique (CTST)	48
4.3.6	Oxidation process	49
4.4	Preparation of Barium Hexaferrite, BHF	50
4.4.1	Selection of raw materials	50
4.4.2	Weighing of the constituent powders	50
4.4.3	Mixing of Fe ₂ O ₃ and BaCO ₃ powders	50
4.4.4	Preparation of barium hexaferrite nanoparticles for BHF-SM and BHF-DM	51
4.5	Preparation of BHF-SM and BHF-DM samples with polymer nanocomposite	51
4.6	Preparation of MWCNTs/BHF hybrid materials	53
4.7	Preparation of Filler (MWCNTs/BHF) loaded with Epoxy Matrix nanocomposite	54
4.8	Sample's Characterizations and measurements	55
4.8.1	X-Ray Diffraction (XRD)	56
4.8.2	Vibrating Sample Magnetometer (VSM)	56
4.8.3	Transmission Electron Microscopy (TEM)	57
4.8.4	Field Emission Scanning Electron Microscope (FESEM)	57
4.8.5	Energy Dispersive X-ray Spectroscopy	58
4.8.6	Raman Spectroscopy	58
4.8.7	Vector Network Analyzer (VNA)	58
4.9	Errors of Measurement	60
5	RESULTS AND DISCUSSION	
5.1	Introduction	61
5.2	M-type barium hexaferrite single milling (BHF-SM)	61

5.2.1	Phase analysis of BHF-SM nanoparticles	61
5.2.2	Microstructural analysis of BHF-SM nanoparticles	66
5.2.3	Elemental analysis of BHF-SM nanoparticles	73
5.2.4	Magnetic properties of BHF-SM nanoparticles	76
5.2.5	Electromagnetic properties of BHF-SM nanocomposites	79
5.3	M-type barium hexaferrite BHF-DM nanoparticles	89
5.3.1	Phase analysis of BHF-DM nanoparticles	89
5.3.2	Microstructural analysis of BHF-DM nanoparticles	93
5.3.3	Elemental analysis of BHF-DM nanoparticles	99
5.3.4	Magnetic properties of BHF-DM nanoparticles	102
5.3.5	Electromagnetic properties of BHF-DM nanoparticles	104
5.4	MWCNTs /BHF-SM hybrid materials	114
5.4.1	Phase analysis	114
5.4.2	Microstructural analysis	115
5.4.3	Raman analysis	118
5.4.4	Elemental analysis	118
5.4.5	Magnetic properties	120
5.4.6	Electromagnetic absorption of MWCNTs/BHF-SM hybrid	121
5.5	MWCNTs/BHF-DM hybrid materials	130
5.5.1	Phase analysis	130
5.5.2	Microstructural analysis	131
5.5.3	Raman analysis	133
5.5.4	Elemental analysis	134
5.5.5	Magnetic properties	135
5.5.6	Electromagnetic absorption of MWCNTs/BHF-SM hybrid	136
5.6	Result summary of the findings	144

6

CONCLUSION

6.1	Conclusion	146
6.2	Recommendation for future works	147

BIBLIOGRAPHY	148
APPENDICES	166
BIODATA OF STUDENT	167
LIST OF PUBLICATIONS	168

LIST OF TABLES

Table		Page
2.1	Comparison of the Hard Ferrites	9
2.2	Examples application of BHF	10
2.3	Microwave absorption properties of various BHF and BHF based camposites	12
2.4	Microwave absorption properties of BHF and BHF/MWCNTs based camposites	20
3.1	Some physical and thermal values and properties for polycrystalline M ferrites	24
3.2	Table 3.2: The summed up of moment for each types of ferrite (M, W, X, Y, Z and U)	27
3.3	Relationship between reflectivity reduction and the absorbed energy	33
4.1	General properties of hematite, magnetite, and wuestite	49
4.2	Details on weight percentages of BHF-SM and BHF-DM nanocomposite loaded into epoxy matrix.	53
4.3	Details on weight percentages of as-synthesized carbon nanotubes loaded into epoxy matrix.	55
4.4	Estimated errors for characterization	60
5.1	Lattice constant a and c , c/a ratio and unit cell volume, V of BHF-SM (800 °C -1400 °C) nanoparticles.	66
5.2	Average particle size of BHF-SM nanoparticles	73
5.3	Saturation magnetization, M_s , coercivity, H_c and Retentivity, M_r of BHF-SM nanoparticles.	78
5.4	Table 5.4: Electromagnetic wave absorption of BHF-SM nanocomposites	88
5.5	Table 5.5: Lattice constant a and c , c/a ratio and unit cell volume, V of BHF-DM nanoparticles	93
5.6	Table 5.6: Average particle size of BHF-DM nanoparticles	99

5.7	Table 5.7: Saturation magnetization, M_s , coercivity, H_c and Retentivity, M_r of BHF-DM nanoparticles.	104
5.8	Electromagnetic wave absorption of BHF-DM nanocomposites	113
5.9	Saturation magnetization, M_s and coercivity, H_c value for BHF-SM (1400 °C) and MWCNTs/BHF-SM hybrid.	120
5.10	Electromagnetic microwave absorption parameters of prepared composite samples at thickness of 1, 2 and 3 mm.	127
5.11	Saturation magnetization, M_s and coercivity, H_c value for BHF-DM (1400 °C) and MWCNTs/BHF-DM hybrid.	136
5.12	Electromagnetic wave absorption properties of BHF-DM (1400 °C) and MWCNTs/BHF-DM hybrid at 1 mm thickness.	142

LIST OF FIGURES

Figure		Page
1.1	Spectrum of electromagnetic waves and microwaves	3
2.1	The reflection loss (RL) of $BaMg_{0.6}Ti_{0.6}Fe_{10.8}O_{19}$ sintered at 800, 900 and 1000 °C	17
2.2	Reflection loss curve (RL) $Ba_{0.6}Sr_{0.4}Fe_{10}MnTiO_{19}$ with filler variation between 20% to 50%	18
2.3	Reflection Loss curve (RL) of $Ba_{0.6}Sr_{0.4}Fe_{12-z}Mn_zO_{19}$ ($z = 0, 1, 2, \text{ and } 3$)	19
3.1	(a) Cross section view of the M-type ferrite ($BaFe_{12}O_{19}$) structure in which the vertical lines are axes of threefold symmetry (b) and (c) perspective views of the M unit cell, (d) The polyhedra of the M unit cell (e) The RSR*S* stacking sequence	26
3.2	Cross section of the BHF structure with the c-axis vertical, and spin orientation of the iron atoms shown by arrows. Net magnetic moment = $4\uparrow = 20 \mu_B$ for BHF the layers containing barium atoms are mirror planes	28
3.3	The hysteresis loop	29
3.4	Propagation of electromagnetic waves	29
3.5	Concept of waves absorber	30
3.6	MAMs absorbing material backed by PEC: Single MAMs absorbing materials and for achieving broadband absorption of EM waves	32
3.7	Typical magnetization (B vs H) curve	35
3.8	Precessional motion of magnetization; a) precession maintained by a microwave field and b) the moment spiraling into line with H as the precessional energy is dissipated	37
3.9	Schematic illustration of the frequency behaviour of ferrites	38
3.10	Debye relaxation model	39

4.1	Figure Procedure of sample preparation of Fe ₂ O ₃	43
4.2	Procedure of samples synthesise and caharacterisation of barium hexaxaferrite single milling (BHF-SM)	44
4.3	Procedure of samples synthesise and caharacterisation of barium hexaxaferrite single milling (BHF-DM)	45
4.4	Procedure of samples synthesised and characterization of MWCNT/BHF-SM and MWCNT/BHF-DM	46
4.5	2 h conventional milling and its accessories	47
4.6	Set up for Magnetic and non-magnetic Separation Technique	48
4.7	Set up for Curie Temperature Separation Technique, CTST	49
4.8	a) BHF-SM after milling for 3 h, b) SPEX 8000D high energy ball milling machine	51
4.9	a) Ferrites powders and epoxy resin mixture, b) Mixing process, c) Sample holder for 1,2 and 3 mm of thickness	52
4.10	Schematic diagram of a chemical vapor deposition (CVD) set up in its simplest form	54
4.11	As-synthesized CNT in the ceramic boat ready to be weighed.	54
4.12	N5227A PNA Network Analyzer (VNA)	59
4.13	Scattering parameter for two port network analyzer	60
5.1(a-g)	X-ray diffraction pattern of BHF-SM nanoparticles	66
5.2a	FESEM image and particle size distribution of BHF-SM sintered at 800 °C	68
5.2b	FESEM image and particle size distribution of BHF-SM sintered at 900 °C	69
5.2c	FESEM image and particle size distribution of BHF-SM sintered at 1000 °C	69
5.2d	FESEM image and particle size distribution of BHF-SM sintered at 1100 °C	70

5.2e	FESEM image and particle size distribution of BHF-SM sintered at 1200 °C	71
5.2f	FESEM image and particle size distribution of BHF-SM sintered at 1300 °C	72
5.2g	FESEM image and particle size distribution of BHF-SM sintered at 1400 °C	73
5.3a	EDX spectrum and fraction of weight percent of BHF-SM nanoparticles sintered at 800 °C	74
5.3b	EDX spectrum and fraction of weight percent of BHF-SM nanoparticles sintered at 900 °C	74
5.3c	EDX spectrum and fraction of weight percent of BHF-SM nanoparticles sintered at 1000 °C	74
5.3d	EDX spectrum and fraction of weight percent of BHF-SM nanoparticles sintered at 1100 °C	75
5.3e	EDX spectrum and fraction of weight percent of BHF-SM nanoparticles sintered at 1200 °C	75
5.3f	EDX spectrum and fraction of weight percent of BHF-SM nanoparticles sintered at 1300 °C	75
5.3g	EDX spectrum and fraction of weight percent of BHF-SM nanoparticles sintered at 1400 °C	76
5.4(a-g)	VSM pattern of BHF-SM (800 °C-1400 °C) nanoparticles.	78
5.5(a, b)	The frequency dependency of (a) real and (b) imaginary part of complex permeability of BHF-SM nanocomposites sintered at 800 °C	80
5.6(a, b)	The frequency dependency of (a) real and (b) imaginary part of complex permeability of BHF-SM nanocomposites sintered at 900 °C	80
5.7(a, b)	The frequency dependency of (a) real and (b) imaginary part of complex permeability of BHF-SM nanocomposites sintered at 1000 °C	80

5.8(a, b)	The frequency dependency of (a) real and (b) imaginary part of complex permeability of BHF-SM nanocomposites sintered at 1100 °C	81
5.9(a, b)	The frequency dependency of (a) real and (b) imaginary part of complex permeability of BHF-SM nanocomposites sintered at 1200 °C	81
5.10(a, b)	The frequency dependency of (a) real and (b) imaginary part of complex permeability of BHF-SM nanocomposites sintered at 1300 °C	81
5.11(a, b)	The frequency dependency of (a) real and (b) imaginary part of complex permeability of BHF-SM nanocomposites sintered at 1400 °C	82
5.12(a, b)	The frequency dependency of (a) real and (b) imaginary part of complex permittivity of BHF-SM nanocomposites sintered at 800 °C	83
5.13(a, b)	The frequency dependency of (a) real and (b) imaginary part of complex permittivity of BHF-SM nanocomposites sintered at 900 °C	83
5.14(a, b)	The frequency dependency of (a) real and (b) imaginary part of complex permittivity of BHF-SM nanocomposites sintered at 1000 °C	84
5.15(a, b)	The frequency dependency of (a) real and (b) imaginary part of complex permittivity of BHF-SM nanocomposites sintered at 1100 °C	84
5.16(a, b)	The frequency dependency of (a) real and (b) imaginary part of complex permittivity of BHF-SM nanocomposites sintered at 1200 °C	84
5.17(a, b)	The frequency dependency of (a) real and (b) imaginary part of complex permittivity of BHF-SM nanocomposites sintered at 1300 °C	85
5.18(a, b)	The frequency dependency of (a) real and (b) imaginary part of complex permittivity of BHF-SM nanocomposites sintered at 1400 °C	85
5.19	The frequency dependency of the <i>RL</i> values for different thickness of BHF-SM nanocomposites sintered at 800 °C at 1, 2 and 3 mm thickness	86

5.20	The frequency dependency of the <i>RL</i> values for different thickness of BHF-SM nanocomposites sintered at 900 °C at 1, 2 and 3 mm thickness	86
5.21	The frequency dependency of the <i>RL</i> values for different thickness of BHF-SM nanocomposites sintered at 1000 °C at 1, 2 and 3 mm thickness	87
5.22	The frequency dependency of the <i>RL</i> values for different thickness of BHF-SM nanocomposites sintered at 1100 °C at 1, 2 and 3 mm thickness	87
5.23	The frequency dependency of the <i>RL</i> values for different thickness of BHF-SM nanocomposites sintered at 1200 °C at 1, 2 and 3 mm thickness	87
5.24	The frequency dependency of the <i>RL</i> values for different thickness of BHF-SM nanocomposites sintered at 1300 °C at 1, 2 and 3 mm thickness	88
5.25	The frequency dependency of the <i>RL</i> values for different thickness of BHF-SM nanocomposites sintered at 1400 °C at 1, 2 and 3 mm thickness	88
5.26	X-ray diffraction pattern of BHF-DM nanoparticles	93
5.27a	FESEM image and particle size distribution of BHF-DM sintered at 800 °C	94
5.27b	FESEM image and particle size distribution of BHF-DM sintered at 900 °C	95
5.27c	FESEM image and particle size distribution of BHF-DM sintered at 1000 °C	96
5.27d	FESEM image and particle size distribution of BHF-DM sintered at 1100 °C	96
5.27e	FESEM image and particle size distribution of BHF-DM sintered at 1200 °C	97
5.27f	FESEM image and particle size distribution of BHF-DM sintered at 1300 °C	98
5.27g	FESEM image and particle size distribution of BHF-DM sintered at 1400 °C	98
5.28a	EDX spectrum and fraction of weight percent of BHF-DM nanoparticles sintered at 800 °C	100

5.28b	EDX spectrum and fraction of weight percent of BHF-DM nanoparticles sintered at 900 °C	100
5.28c	EDX spectrum and fraction of weight percent of BHF-DM nanoparticles sintered at 1000 °C	100
5.28d	EDX spectrum and fraction of weight percent of BHF-DM nanoparticles sintered at 1100 °C	101
5.28e	EDX spectrum and fraction of weight percent of BHF-DM nanoparticles sintered at 1200 °C	101
5.28f	EDX spectrum and fraction of weight percent of BHF-DM nanoparticles sintered at 1300 °C	101
5.28g	EDX spectrum and fraction of weight percent of BHF-DM nanoparticles sintered at 1400 °C	102
5.29 (a-g)	VSM pattern of BHF-DM (800 °C-1400 °C) nanoparticles.	103
5.30(a, b)	The frequency dependency of (a) real and (b) imaginary part of complex permeability of BHF-DM nanocomposites sintered at 800 °C	105
5.31(a, b)	The frequency dependency of (a) real and (b) imaginary part of complex permeability of BHF-DM nanocomposites sintered at 900 °C	105
5.32(a, b)	The frequency dependency of (a) real and (b) imaginary part of complex permeability of BHF-DM nanocomposites sintered at 1000 °C	105
5.33(a, b)	The frequency dependency of (a) real and (b) imaginary part of complex permeability of BHF-DM nanocomposites sintered at 1100 °C	106
5.34(a, b)	The frequency dependency of (a) real and (b) imaginary part of complex permeability of BHF-DM nanocomposites sintered at 1200 °C	106
5.35(a, b)	The frequency dependency of (a) real and (b) imaginary part of complex permeability of BHF-DM nanocomposites sintered at 1300 °C	106
5.36(a, b)	The frequency dependency of (a) real and (b) imaginary part of complex permeability of BHF-DM nanocomposites sintered at 1400 °C	107

5.37(a, b)	The frequency dependency of (a) real and (b) imaginary part of complex permittivity of BHF-DM nanocomposites sintered at 800 °C	108
5.38(a, b)	The frequency dependency of (a) real and (b) imaginary part of complex permittivity of BHF-DM nanocomposites sintered at 900 °C	108
5.39(a, b)	The frequency dependency of (a) real and (b) imaginary part of complex permittivity of BHF-DM nanocomposites sintered at 1000 °C	108
5.40(a, b)	The frequency dependency of (a) real and (b) imaginary part of complex permittivity of BHF-DM nanocomposites sintered at 1100 °C	109
5.41(a, b)	The frequency dependency of (a) real and (b) imaginary part of complex permittivity of BHF-DM nanocomposites sintered at 1200 °C	109
5.42(a, b)	The frequency dependency of (a) real and (b) imaginary part of complex permittivity of BHF-DM nanocomposites sintered at 1300 °C	109
5.43(a, b)	The frequency dependency of (a) real and (b) imaginary part of complex permittivity of BHF-DM nanocomposites sintered at 1400 °C	110
5.44	The frequency dependency of the RL values for different thickness of BHF-DM nanocomposites sintered at 800 °C at 1, 2 and 3 mm thickness	110
5.45	The frequency dependency of the RL values for different thickness of BHF-DM nanocomposites sintered at 900 °C at 1, 2 and 3 mm thickness	111
5.46	The frequency dependency of the RL values for different thickness of BHF-DM nanocomposites sintered at 1000 °C at 1, 2 and 3 mm thickness	111
5.47	The frequency dependency of the RL values for different thickness of BHF-DM nanocomposites sintered at 1100 °C at 1, 2 and 3 mm thickness	111
5.48	The frequency dependency of the RL values for different thickness of BHF-DM nanocomposites sintered at 1200 °C at 1, 2 and 3 mm thickness	112

5.49	The frequency dependency of the RL values for different thickness of BHF-DM nanocomposites sintered at 1300 °C at 1, 2 and 3 mm thickness	112
5.50	The frequency dependency of the RL values for different thickness of BHF-DM nanocomposites sintered at 1400 °C at 1, 2 and 3 mm thickness	112
5.51	XRD pattern of (a)BHF-SM (1400 °C), (b) MWCNTs/BHF-SM hybrid via CVD.	115
5.52	FESEM images of (a) BHF-SM (1400 °C), (b) FESEM images of MWCNTs/BHF-SM hybrid (c) enlarge image of BHF-SM (1400 °C) nanoparticles	117
5.53	HRTEM image of MWCNTs/BHF-SM hybrid	117
5.54	Raman spectra of MWCNTs/BHF-SM hybrid.	118
5.55	EDX pattern of (a) BHF-SM (1400 °C) and (b) MWCNTs/BHF-SM hybrid.	119
5.56	EDX an elemental mapping figures distribution of MWCNTs/BHF-SM hybrid	120
5.57	Room temperature hysteresis loop of BHF-SM (1400 °C) and MWCNTs/BHF-SM hybrid	121
5.58	Frequency dependency of (a) real and (b) imaginary parts of the complex permeability (μ_r) values for BHF-SM (1400 °C) and MWCNTs/BHF-SM hybrid with different filler contents (2, 4, 6, 8 and 10 wt%) and with thicknesses of d = 1 mm	122
5.59	Frequency dependency of (a) real and (b) imaginary parts of the complex permeability (μ_r) values for BHF-SM (1400 °C) and MWCNTs/BHF-SM hybrid with different filler contents (2, 4, 6, 8 and 10 wt%) and with thicknesses of d = 2 mm	122
5.60	Frequency dependency of (a) real and (b) imaginary parts of the complex permeability (μ_r) values for BHF-SM (1400 °C) and MWCNTs/BHF-SM hybrid with different filler contents (2, 4, 6, 8 and 10 wt %) and with thicknesses of d = 3 mm	123
5.61	Frequency dependency of (a) real and (b) imaginary parts of the complex permittivity (ϵ_r) values for BHF-SM (1400 °C) and MWCNTs/BHF-SM hybrid with different filler	124

	contents (2, 4, 6, 8 and 10 wt%) and with thicknesses of $d = 1$ mm	
5.62	Frequency dependency of (a) real and (b) imaginary parts of the complex permittivity (ϵ_r) values for BHF-SM (1400 °C) and MWCNTs/BHF-SM hybrid with different filler contents (2, 4, 6, 8 and 10 wt%) and with thicknesses of $d = 2$ mm	124
5.63	Frequency dependency of (a) real and (b) imaginary parts of the complex permittivity (ϵ_r) values for BHF-SM (1400 °C) and MWCNTs/BHF-SM hybrid with different filler contents (2, 4, 6, 8 and 10 wt%) and with thicknesses of $d = 3$ mm.	124
5.64(a, b, c)	Frequency dependency of reflection loss (RL) for BHF-SM (1400 °C) and MWCNTs/BHF-SM hybrid with different filler contents (2, 4, 6, 8 and 10 wt%) and a thickness of $d = 1, 2$ and 3 mm	126
5.65	Frequency dependency of (a) impedance matching and (b) attenuation constant values for BHF-SM (1400 °C) and MWCNTs/BHF-SM hybrid with different filler contents (2, 4, 6, 8 and 10 wt%) and a thickness of $d = 2$ mm	129
5.66	Frequency dependency of (a) dielectric loss tangent ($\tan \delta\epsilon$) and (b) magnetic loss tangent ($\tan \delta\mu$) values for BHF-SM (1400 °C) MWCNTs/BHF-SM hybrid with different filler contents (2, 4, 6, 8 and 10 wt%) and with a thickness of $d = 2$ mm	129
5.67	Complex Impedance Cole-Cole Plot of the BHF-SM (1400 °C) and MWCNTs/BHF-SM hybrid with different filler contents (2, 4, 6, 8 and 10 wt%) and a thickness of $d = 2$ mm	129
5.68	XRD spectra of (a) BHF-DM (1400 °C) and (b) MWCNTs/BHF-DM hybrid	130
5.69	FESEM images of (a) BHF-DM (1400 °C), (b) FESEM images of MWCNTs/BHF-DM hybrid and (c) enlarge image of BHF-DM (1400 °C) nanoparticles	132
5.70	HRTEM image of MWCNTs/BHF-DM hybrid	133
5.71	Raman spectra of MWCNTs/BHF-DM hybrid	133
5.72	EDX pattern of (a) BHF-DM (1400 °C) and (b) MWCNTs/BHF-DM hybrid	134

5.73	EDX an elemental mapping figures distribution of MWCNTs/BHF-DM hybrid	135
5.74	Room temperature hysteresis loop of BHF-DM (1400 °C) and MWCNTs/BHF-DM hybrid	136
5.75	Frequency dependency of (a) real and (b) imaginary parts of the complex permittivity (ϵ_r) values for BHF-DM (1400 °C) and MWCNTs/BHF-DM hybrid with different filler contents (2, 4, 6, 8 and 10 wt%) and with thicknesses of $d = 1$ mm	137
5.76	Frequency dependency of (a) real and (b) imaginary parts of the complex permittivity (ϵ_r) values for BHF-DM (1400 °C) and MWCNTs/BHF-DM hybrid with different filler contents (2, 4, 6, 8 and 10 wt%) and with thicknesses of $d = 2$ mm	137
5.77	Frequency dependency of (a) real and (b) imaginary parts of the complex permittivity (ϵ_r) values for BHF-DM (1400 °C) and MWCNTs/BHF-DM hybrid with different filler contents (2, 4, 6, 8 and 10 wt%) and with thicknesses of $d = 3$ mm	138
5.78	Frequency dependency of (a) real and (b) imaginary parts of the complex permeability (μ_r) values for BHF-DM (1400 °C) and MWCNTs/BHF-DM hybrid with different filler contents (2, 4, 6, 8 and 10 wt%) and with thicknesses of $d = 1$ mm	139
5.79	Frequency dependency of (a) real and (b) imaginary parts of the complex permeability (μ_r) values for BHF-DM (1400 °C) and MWCNTs/BHF-DM hybrid with different filler contents (2, 4, 6, 8 and 10 wt%) and with thicknesses of $d = 2$ mm	139
5.80	Frequency dependency of (a) real and (b) imaginary parts of the complex permeability (μ_r) values for BHF-DM (1400 °C) and MWCNTs/BHF-DM hybrid with different filler contents (2, 4, 6, 8 and 10 wt%) and with thicknesses of $d = 3$ mm	139
5.81(a, b, c)	Frequency dependency of reflection loss (RL) for BHF-DM (1400 °C) and MWCNTs/BHF-DM hybrid with different filler contents (2, 4, 6, 8 and 10 wt%) and a thickness of $d = 1, 2$ and 3 mm	141

5.82	Frequency dependency of (a) impedance matching and (b) attenuation constant values for BHF-DM (1400 °C) and MWCNTs/BHF-DM hybrid with different filler contents (2, 4, 6, 8 and 10 wt%) and a thickness of $d = 2$ mm	143
5.83	Frequency dependency of (a) dielectric loss tangent ($\tan \delta\epsilon$) and (b) magnetic loss tangent ($\tan \delta\mu$) values for BHF-DM (1400 °C) and MWCNTs/BHF-DM hybrid with different filler contents (2, 4, 6, 8 and 10 wt%) and with a thickness of $d = 2$ mm	144
5.84	Complex Impedance Cole-Cole plot of the BHF-DM (1400 °C) and MWCNTs/BHF-DM hybrid with different filler contents (2, 4, 6, 8 and 10 wt%) and a thickness of $d = 2$ mm	144

LIST OF ABBREVIATIONS

BHF	Barium Hexaferrite
BHF-SM	Barium Hexaferrite Single Milling
BHF-DM	Barium Hexaferrite Double Milling
BPR	Ball to powder weight ratio
CNTs	Carbon Nanotubes
CVD	Chemical vapour deposition
EM	Electromagnetic
EDX	Energy Dispersive X-ray
FeSEM	Field Emission Scanning Electron Microscope
HEBM	High Energy Ball Milling
HRTEM	High Resolution Transmission electron microscope
Ku-band	12-18 GHz
MWCNTs	Multi-Walled Carbon Nanotubes
MAMs	Microwaves absorbing materials
<i>RL</i>	Reflection loss
VNA	Vector Network Analyzer
VSM	Vibrating Sample Magnetometer
XRD	X-ray Diffraction
X-band	8-12 GHz
<i>a, c</i>	Lattice parameter
Ba	Barium
<i>B</i>	Magnetic field
CO ₃	Carbonate

dB	Decibel
ϵ'	Real permittivity
ϵ''	Imaginary permittivity
ϵ_0	Free space permittivity
Fe	Iron
f_r	Resonance frequency
H_A	Anisotropy field for c-axis anisotropy
H	Applied magnetic field
H_c	Coercivity field
K_1, K_2	Magnetocrystalline anisotropy
M_s	Saturated Magnetization
M_r	Retentivity Magnetization
O	Oxygen
T_c	Curie temperature
t	Thickness
μ'	Real permeability
μ''	Imaginary permeability
μ_0	Free space permeability
V	Unit cell volume
wt %	Weight percentage
γ	Gyromagnetic ratio
Z_0	Free space impedance
Z_{in}	Normalized input impedance
2θ	2 theta degree

CHAPTER 1

INTRODUCTION

1.1 Background of the study

There has been a growing and widespread interest in microwave absorbing material technology. As the name implies, microwave absorbing materials (MAMs) are coatings whose electrical and/or magnetic properties have been altered to allow absorption of microwave energy at discrete or broadband frequencies, which work at frequencies between 300 MHz and 300 GHz. The arrangement of all forms of electromagnetic waves based on their wavelengths and frequencies covers a very low range of energy to very high energy called the electromagnetic wave spectrum, as shown in Figure 1.1. Therefore, microwave absorbing material has the two most prominent applications for electromagnetic wave interference (EMI), including military and commercial electronics. The application of absorbers in military and defense (Saville, 2005; Vinoy et al., 1996), this microwave absorber is used to coat or paint defense equipment and installations such as stealth aircraft, warships, and military uniforms, particularly for the guards. to reduce interference while, in commercial electronics can be found in wireless LAN devices, network servers, VSAT transceivers, radios, and other high-frequency devices. However, with continuous exposure to this electromagnetic radiation, pollution of electromagnetic interference can disrupt various systems and equipment for civil and military applications (Wang et al., 2015). In the electronics field, microwave absorbers are used to reduce the presence of EMI (Eswaraiah et al., 2011; Wu and Li, 2011). In general, electronic components that work at high frequencies often experience problems such as frequency signal leakage. Therefore, EMI will not be present if the electronic device is open or not in a secure medium. However, signals traveling in a closed medium will be reflected in the device. This will cause the energy to increase in phase at specific frequencies due to the appearance of EMI emitted in the form of noise, which then interferes with the performance of these electronic devices. Then, after microwave absorbers protect the closed media, the effect of EMI can be avoided.

In a radar system, an electromagnetic wave in the microwave frequency range is transmitted continuously in all directions by the transmitter. If an object is affected by this wave, the signal will be reflected by the object and received back by the recipient. This reflection signal will provide information that there is a close object that the radar screen will display. Radar (radio detection and ranging) is a microwave system helpful in detecting and measuring distances and making maps of an object. The radar waves emitted can detect the presence of an object. The radar concept measures the distance from the sensor to the target. The length is obtained by measuring the time needed by the radar wave during its propagation from the sensor to the mark and back to the sensor again. The

measured distance based on the time required by the electromagnetic waves emanating from the target is then reflected by the radar sensor. The target can reflect electromagnetic waves so that the radar can detect the existence of these objects. When an electromagnetic (EM) wave is targeted to the material surface, part of the EM wave is reflected off the surface or into the surface and absorbed by the material or transmitted through the material. Therefore, for good microwave absorption, two essential conditions must-have, which are:

- i) the intrinsic impedance of the material is equal to the free space impedance, and
- ii) the electromagnetic wave can penetrate and be weakened in the material (Meng et al., 2009).

EM wave energy can be absorbed entirely and dissipated into heat through magnetic losses and/or dielectric loss if the characteristic impedance of free space is matched with the input characteristic impedance of an absorber. For good absorbing performance, the materials are needed with high microwave permeability, high magnetic loss, a good form of frequency dependence of permeability, and a proper ratio between permeability and permittivity (Lagarkov and Rozanov, 2009). In addition, the fabricated absorbing material should have electric and/or magnetic dipoles to interact with the electromagnetic fields in the radiation. Thus, a microwave absorbing material can be classified as magnetic, dielectric, or hybrid (a combination of magnetic and dielectric) since pure dielectric or magnetic materials are insufficient for absorbing radiation energy. Like virtually everything else in the microwave engineering world, absorber design is an impedance matching problem, in this case matching the impedance of a metal surface ($Z = 0$) to the impedance of free space ($Z = 377$ ohms) (Dixon, 2012). If the impedance at the material's surface is equal to 377 ohms, the wave will be completely absorbed by the material.

Among the various types of absorbers, magnetic materials, generally known as ferrites, have shown the potential due to significant losses in the vicinity of ferromagnetic resonance (FMR) and dielectric relaxation peaks. Ferrites are found in different structures such as spinel ferrites, garnets, and hexagonal ferrites (Meena et al., 2010). Garnet ferrites have low magnetization and magnetic field anisotropy saturation values. Hence their implementations are limited to a maximum of 1–2 GHz (Harris et al., 2009). Spinel ferrites are also commonly used as microwave absorbers due to their high magnetic losses and resistivity. However, spinel ferrites are not effective in the frequency range of microwaves due to intrinsic restrictions imposed by the incidence of their normal FMR below 1 GHz (Ahmad et al., 2012). Xie et al. (2007) designed a thin wideband microwave absorber using NiCoZn spinel ferrites. For the radio frequency and low-frequency part of the microwave range (less than a few hundred MHz), spinel ferrites can meet these requirements. However, ferrites with substantially higher magnetic anisotropy are required within the gigahertz frequency range. Ferrites also have attractive and repulsive forces properties of magnetic materials. For this purpose, we need to switch to hexagonal ferrites,

having the magnetoplumbite structure. For higher frequencies (above few gigahertz), hexagonal ferrites and composites with ferromagnetic inclusions provide noticeable permeability values. In the frequency range from 10 to 30 GHz, important for 5G applications, hexaferrite and composites with hexaferrite inclusions are promising materials (Sai et al., 2017). However, ferrites alone suffer from weak absorption, heavy mass density, lower dielectric losses, and narrow absorption band (Yue et al., 2012). To undertake these shortcomings, composites of different ferrites with carbon nanotubes MWCNTs, and polymers have been widely explored (Abbas et al., 2016; Wang et al., 2014; Wang et al., 2013). MWCNTs, when used as a dielectric absorber in MWCNTs/polymer/metal ferrite nanocomposites, have fascinated extensive considerations owing to their one-dimensional microstructure, outstanding mechanical, thermal, and electrical properties, high Young's modulus, large surface area, high aspect ratio, low density, high strength and flexibility (Phan et al., 2016; Zhu et al., 2015; Tan et al., 2015). These characteristics are good to use for the best potential microwave absorber material.

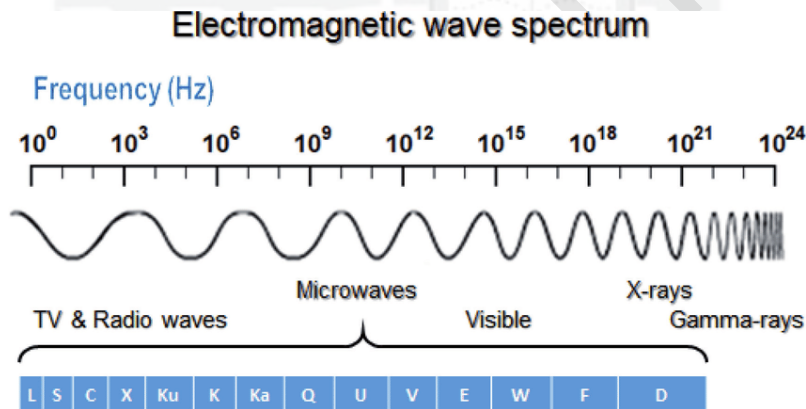


Figure 1.1: Spectrum of electromagnetic waves and microwaves (Adi et al., 2019)

1.2 A potential of raw material waste mill scale

Mill scale is a waste product, often present on raw steel and is frequently mistaken for a blue-colored. Mill scale is a type of iron oxide formed on the steel's surface during the hot-rolling process (Nadhirah et al., 2015; Legodi and De Waal, 2007). The very high surface temperature combined with high roller pressures results in a smooth, bluish-grey surface. Mill scale is less reactive (more "noble") than the steel underneath, and consistent with the behavior of two dissimilar metals when in contact, the more reactive metal (in this case steel) will oxidize (rust) at the expense of the less reactive metal (mill scale). The waste mill scales in the form of scales, and it can "pop off" the surface, cracking the coating and allowing moisture to penetrate. In this research, hematite is produced from mill scale as the raw materials to produced barium hexagonal

ferrite. The raw mill scale went through the milling and purification process to make high purity hematite (Fe_2O_3) powder as starting material for preparing barium hexagonal ferrite. The principal reason for utilizing waste mill scales product is to reduce the production cost because it is cheap, reutilizes waste materials, is abundant and readily available in the market.

1.3 Potential Multi-walled Carbon Nanotubes (MWCNTs) as microwave absorbing materials

MWCNTs composites have many advantages due to their ability to adapt to the dielectric properties and to possess lightweight structures without reducing the mechanical properties. MWCNTs may be metallic or semiconducting, which rest on their geometry, chirality, and diameter. The electrical conductivity of MWCNTs is reported to be $>10^6\text{--}7\text{ Sm}^{-1}$ (Afrin et al., 2016). Since the discovery of MWCNTs, their use as reinforcing filler in various materials has been ever-increasing (Ghasemi et al., 2011). However, multi-walled carbon nanotubes (MWCNTs) conceive more defects than single-wall carbon nanotubes (SWCNTs) because of their complex structure, higher permittivity, and absorption (reflection loss, RL), primarily due to relaxation of dielectrics. In addition, MWCNTs surface is nonreactive, so to improve their dispersion, interfacial bonding, surface reactivity, and open their tip walls, covalent or non-covalent functionalization is carried out, and metal ferrite nanoparticles can be coated to improve their conductivity and to absorb properties (Rehman et al., 2013). Previous research has shown that various percent of MWCNTs introduction into soft and hard ferrite via the sol-gel method, in situ precipitation, hydrothermal, and in-situ solvothermal has significantly improved the microwave absorption characteristics. Furthermore, the introduction of MWCNTs into ferrite samples has increased the conductivity (Cao et al., 2007; Akhtar et al., 2011; Ghasemi et al., 2011).

1.4 Problem Statement

In the past several decades, studies on BHF by pure materials have been reported in ferrite literature. Instead, fabricate the BHF using a recycled waste mill scale was still investigated. However, there was less report from literature has been done on this work. Steel waste products are collected from the steel industry in Malaysia. It has a high iron content (Fe) and gives us the challenge to purify and recycle the powder to produce BHF. This project will highlight the low-cost ferrite fabrication from the steel waste product. The particle size of the materials is also one of the factors to enhance microwave absorption properties. The smaller nanoparticles of BHF would result in a huge absorption ability (Reflection Loss) in a wide frequency range. In general, the larger particle size of materials would degrade the electromagnetic wave characteristics since the larger particle size have a smaller surface area per unit volume with fewer surface atoms. So that, in this research, double milling process after sintering

was introduced via the high-energy ball milling method (HEBM). Hence, in this present work, the evolutions of BHF at various sintering temperatures were also investigated. With the vast utilization of these microwave absorbing materials, it is generally accepted to recognize that microwave absorbing material is a material that can weaken the energy of electromagnetic waves. However, these microwave absorbing materials can externally reduce or even eliminate reflections or transmissions from particular objects and can be used internally to minimize oscillations caused by resonance cavities. Moreover, the fundamental scientific inquiry of the structural, magnetic, microstructure, electromagnetic, and microwave property evolution has been neglected. In this research, MWCNTs will be introduced as one way to improve microwave absorption characteristics with wideband frequency capability. MWCNTs submit into hard ferrite (BHF) via Chemical vapor Deposition (CVD), whereas BHF is used as a catalyst. The MWCNTs/BHF hybrid, chemically attached, will increase the energy transfer from one medium to another medium. Thus, hypothetically, the EM wave absorption becomes more efficient. According to the problem statement, the hypothesis of this research project is the modification hematite extracted from mill scale waste. Besides, smaller size (nanosize) of BHF result in the enhancement of the microwave absorption (RL) with introducing double milling step after sintering via HEBM method. In addition, the introducing of MWCNTs that submit into BHF as a hybridization sample via Chemical vapor Deposition (CVD) will contribute to the microwave absorption characteristics. Hence, in this research work, structural, microstructure, magnetic and electromagnetic absorption properties for MAMs are studied aiming to improve their electromagnetic and microwave absorbing performance in terms of high absorption level, operating in a broadband frequency range, have simple coating-layer structure, thin and lightweight as possible.

1.5 Objectives

1.5.1 Main research project objective

The interest of this research is to study electromagnetic absorption characteristics as microwave absorbing materials and to understand the underlying scientific mechanisms that enable them to exhibit high-level absorption (≤ -30 dB) in the (8 – 18 GHz) frequency range.

1.5.2 Work-phase Objectives

Hence this research work embarks on the following work-phase objectives which are:

- i. To synthesize BHF single milling and double milling by High Energy Ball Milling (HEBM) and sintered at various sintering temperatures.

- ii. To synthesize MWCNTs/BHF with different filler content (2, 4, 6, 8, and 10 wt%).
- iii. To analyze the magnetic, dielectric, and reflection loss properties (S_{11} and S_{21} parameter) in obtaining BHF materials and MWCNTs/BHF used as an absorber with an ultimate performance reflection loss (≤ -30 dB).

1.6 Limitations of the study

There are a few limitations concerning this research:

- For M-type of BHF and MWCNTs/BHF hybrid, the measurement was only limited for RL since it was only prepared for evaluation to find the best and optimized absorbing materials.
- The measurement was carried out only in the X-band (8-12 GHz) and Ku band (12-18 GHz) frequency, respectively, due to the restriction in experimental equipment constrained.

1.7 Outlines of the thesis

Background of the study in this work, selection of M-type materials, a potential of raw material waste mill scale, a potential MWCNTs as MAMs, the aim of study, objectives, and limitation of the study in this work has been discussed in Chapter 1. The literature review regarding microwave absorbing materials has been detailed in Chapter 2. A brief theory on the structure and properties of microwave absorbing materials is discussed in Chapter 3. Further on in Chapter 4, the methodology and characterization of this work have been explicitly detailed. All the samples reported in this work have been explained in Chapter 5. Lastly, in Chapter 6, the conclusion based on the discovered results and some suggestions has been proposed. At the end of this thesis, the bibliography, appendices, author biography, and publication list of publications are listed, respectively.

BIBLIOGRAPHY

- Alam, R. S., Moradi, M., Rostami, M., Nikmanesh, H., Moayedi, R., & Bai, Y. (2015). Structural, magnetic and microwave absorption properties of doped Ba-hexaferrite nanoparticles synthesized by co-precipitation method. *Journal of Magnetism and Magnetic Materials*, 381, 1-9.
- Afghahi, S. S. S., Jafarian, M., & Stergiou, C. A. (2016). X-band microwave absorbing characteristics of multicomponent composites with magnetodielectric fillers. *Journal of Magnetism and Magnetic Materials*, 419, 386-393.
- Awadallah, A. M., & Sami, M. (2014). Effects of preparation conditions and metal ion substitutions for barium and iron on the properties of M-type barium hexaferrites (Doctoral dissertation, The University of Jordan).
- Abdollahi, F., Yousefi, M., Hekmati, M., Khajehnezhad, A., & Seyyed Afghahi, S. S. (2019). Magnetic and microwave absorption properties of barium hexaferrite doped with La^{3+} and Gd^{3+} . *Journal of Nanostructures*, 9(3), 579-586.
- Azis, R. A. S., Hashim, M., Azmi, Z., Hassan, J., Daud, N., Mohd Shahrani, N. M., & Siang, P. C. (2016). Magnetic properties and microstructures of cobalt substituted barium hexaferrites derived from steel waste product via mechanical alloying technique. In *Materials Science Forum* (Vol. 846, pp. 388-394). Trans Tech Publications Ltd.
- Azis, R. A. S., Hashim, M., Saiden, N. M., Daud, N., & Shahrani, N. M. M. (2015). Study the iron environments of the steel waste product and its possible potential applications in ferrites. In *Advanced Materials Research* (Vol. 1109, pp. 295-299). Trans Tech Publications Ltd.
- Ahmad, M., Grössinger, R., Kriegisch, M., Kubel, F., & Rana, M. U. (2012). Magnetic and microwave attenuation behavior of Al-substituted Co_2W hexaferrites synthesized by sol-gel autocombustion process. *Current Applied Physics*, 12(6), 1413-1420.
- Abbas, S. M., Ahmad, N., Rana, U. A., Khan, S. U. D., Hussain, S., & Nam, K. W. (2016). High rate capability and long cycle stability of Cr_2O_3 anode with CNTs for lithium ion batteries. *Electrochimica Acta*, 212, 260-269.
- Akhtar, M. N., Yahya, N., Koziol, K., & Nasir, N. (2011). Synthesis and characterizations of $\text{Ni}_{0.8}\text{Zn}_{0.2}\text{Fe}_2\text{O}_4$ -MWCNTs composites for their application in sea bed logging. *Ceramics International*, 37(8), 3237-3245.
- Afrin, R., Abbas, S. M., Shah, N. A., Mustafa, M. F., Ali, Z., & Ahmad, N. (2016).

Effect of Varying Inert Gas and Acetylene Concentration on the Synthesis of Carbon Nanotubes. *Journal of nanoscience and nanotechnology*, 16(3), 2956-2959.

Adi, W. A., Yunasfi, Y., Mashadi, M., Winatapura, D. S., Mulyawan, A., Sarwanto, Y., & Taryana, Y. (2019). Metamaterial: Smart Magnetic Material for Microwave Absorbing Material. *Electromagnetic Fields and Waves*, 1-18.

Akhterov, M. V, *Microwave Absorption in Nanostructures*, B. Sc. Thesis. University of California, Santa Cruz, (2010).

Afzali, A., Mottaghitalab, V., Afghahi, S. S. S., Jafarian, M., & Atassi, Y. (2017). Electromagnetic properties of absorber fabric coated with BaFe₁₂O₁₉/MWCNTs/PANi nanocomposite in X and Ku bands frequency. *Journal of Magnetism and Magnetic Materials*, 442, 224-230.

Aguiar, P. M., Jacquinet, J. F., & Sakellariou, D. (2009). Experimental and numerical examination of eddy (Foucault) currents in rotating micro-coils: Generation of heat and its impact on sample temperature. *Journal of Magnetic Resonance*, 200(1), 6-14.

Adebayo, L. L., Soleimani, H., Yahya, N., Abbas, Z., Wahaaba, F. A., Ayinlaa, R. T., and Ali, H. (2020). Recent advances in the development of Fe₃O₄-Based microwave absorbing materials. *Ceramics International*, 46, 1249–1268.

Adelskold, V. (1938). *Arkiv Kemi Miner.*

Baniasadi, A., Ghasemi, A., Nemati, A., Ghadikolaei, M. A., & Paimozd, E. Batlle, X., Garcia del Muro, M., Tejada, J., Pfeiffer, H., Görnert, P., and Sinn, E. (1993). Magnetic study of M-type doped barium ferrite nanocrystalline powders. *Journal of Applied Physics*, 74(5), 3333-3340.

Brinker, C. J., & Scherer, G. W. (1990). *Sol-Gel Science, The Phys Chem. Sol-Gel Processing*, ISBN 0121349705.

Braun, P. B., Hornstra, J., & Leenhouts, J. I. (1957). *Philips Res. Rep.*, 12, 491-548.

Bahadur, A., Saeed, A., Iqbal, S., Shoaib, M., Ahmad, I., ur Rahman, M. S., & Hussain, W. (2017). Morphological and magnetic properties of BaFe₁₂O₁₉ nanoferrite: A promising microwave absorbing material. *Ceramics International*, 43(9), 7346-7350.

Bsoul, I., & Mahmood, S. H. (2010). Magnetic and structural properties of BaFe_{12-x}GaxO₁₉ nanoparticles. *Journal of Alloys and Compounds*, 489(1), 110-114.

- Belov, K. P., Jergin, Y. V., Koroleva, L. I., Levitin, R. Z., & Pedko, A. V. (1965). Die magnetokristalline Anisotropie hexagonaler ferromagnetischer Stoffe in der Nähe des Curie-Punktes. *physica status solidi (b)*, 12(1), 219-224.
- Cao, H. B., Zhao, Z. Y., Lee, M., Choi, E. S., McGuire, M. A., Sales, B. C., & Mandrus, D. G. (2015). High pressure floating zone growth and structural properties of ferrimagnetic quantum paraelectric BaFe₁₂O₁₉. *Apl Materials*, 3(6), 062512.
- Chiu, S. C., Yu, H. C., & Li, Y. Y. (2010). High electromagnetic wave absorption performance of silicon carbide nanowires in the gigahertz range. *The Journal of Physical Chemistry C*, 114(4), 1947-1952.
- Cao, H., Zhu, M., Li, Y., Liu, J., Ni, Z., & Qin, Z. (2007). A highly coercive carbon nanotube coated with Ni_{0.5}Zn_{0.5}Fe₂O₄ nanocrystals synthesized by chemical precipitation–hydrothermal process. *Journal of solid state chemistry*, 180(11), 3218-3223.
- Casimir, H. B. G., Smit, J., Enz, U., Fast, J. F., Wijn, H. P. J., Gorter, E. W., & De Jong, J. J. (1959). Rapport sur quelques recherches dans le domaine du magnétisme aux laboratoires Philips. *J. Phys. Radium*, 20(2-3), 360-373.
- Chen, L. F., Ong, C. K., Neo, C. P., Varadan, V. V., & Varadan, V. K. (2004). *Microwave electronics: measurement and materials characterization*. John Wiley & Sons.
- Cherradi, D. G., Provost, J., & Raveau, B. (1994). Electric and magnetic field contributions to the microwave sintering of ceramics. *Electroceramics IV*, 2, 1219-12.
- Cao, Z., Wang, Z., Yoshikawa, N., & Taniguchi, S. (2008). Microwave heating origination and rapid crystallization of PZT thin films in separated H field. *Journal of Physics D: Applied Physics*, 41(9), 092003.
- Coffey, W. T., Crothers, D. S. F., Dormann, J. L., Kalmykov, Y. P., Kennedy, E. C., & Wernsdorfer, W. (1998). Thermally activated relaxation time of a single domain ferromagnetic particle subjected to a uniform field at an oblique angle to the easy axis: Comparison with experimental observations. *Physical review letters*, 80(25), 5655.
- Cheng, J., Roy, R., & Agrawal, D. (2002). Radically different effects on materials by separated microwave electric and magnetic fields. *Materials Research Innovations*, 5(3-4), 170-177.
- Chen, M., & Nikles, D. E. (2002). Synthesis, Self-Assembly, and Magnetic Properties of FexCoy Pt100-x-y Nanoparticles. *Nano Letters*, 2(3), 211-214.

- Cao, M. S., Wang, X. X., Zhang, M., Shu, J. C., Cao, W. Q., Yang H. J., Fang, X. Y. and Yuan, J. (2019b). Electromagnetic Response and Energy Conversion for Functions and Devices in Low-Dimensional Materials. *Advanced Functional Materials*, 29(25), 1807398.
- Chang, S., Kangning, S., & Pengfei, C. (2012). Microwave absorption properties of Ce-substituted M-type barium ferrite. *Journal of Magnetism and Magnetic Materials*, 324(5), 802-805.
- Delacotte, C., Whitehead, G. F. S., Pitcher, M. J., Robertson, C. M., Sharp, P. M., Dyer, M. S., & Rosseinsky, M. J. (2018). Structure determination and crystal chemistry of large repeat mixed-layer hexaferrites. *IUCrJ*, 5(6), 681-698.
- Deng, L., Zhao, Y., Xie, Z., Liu, Z., Tao, C., & Deng, R. (2018). Magnetic and microwave absorbing properties of low-temperature sintered BaZrxFe(12-x)O₁₉. *RSC Advances*, 8(73), 42009-42016.
- Dupuis, A. C. (2005). The catalyst in the CCVD of carbon nanotubes—a review. *Progress in materials science*, 50(8), 929-961.
- Dixon, P. (2012). Theory and application of RF/microwave absorbers. In *Emerson & Cuming Microwave Products*.
- Dresselhaus MS, Dresselhaus G, Avouris Ph (Eds) (2001). In: *Carbon nanotubes: synthesis, structure, properties, and applications*. Berlin: Springer-Verlag; 12–51.
- Drofenik, M., Ban, I., Makovec, D., Žnidaršič, A., Jagličić, Z., Hanžel, D., & Lisjak, D. (2011). The hydrothermal synthesis of super-paramagnetic barium hexaferrite particles. *Materials Chemistry and Physics*, 127(3), 415-419.
- Daud, N., Azis, R. A. S., Hashim, M., Matori, K. A., Hassan, J., Saiden, N. M., & Mohd Shahrani, N. M. (2016). Preparation and characterization of Sr_{1-x}NdxFe₁₂O₁₉ derived from steel-waste product via mechanical alloying. In *Materials Science Forum* (Vol. 846, pp. 403-409). Trans Tech Publications Ltd.
- Duan, Y., Cui, Y., Zhang, B., Ma, G., & Tongmin, W. (2019). A novel microwave absorber of FeCoNiCuAl high-entropy alloy powders: adjusting electromagnetic performance by ball milling time and annealing. *Journal of Alloys and Compounds*, 773, 194-201.
- Dong, S., Xu, M., Wei, J., Yang, X., & Liu, X. (2014). The preparation and wide frequency microwave absorbing properties of tri-substituted-bisphthalonitrile/Fe₃O₄ magnetic hybrid microspheres. *Journal of magnetism and magnetic materials*, 349, 15-20.
- Duan, Y., & Guan, H. (2016). *Microwave absorbing materials*. CRC Press.

- Ervens. W and Wilmesmeier. H (1990), Ullmann's Encyclopedia of Industrial Chemistry, Fifth Edition, p1-51.
- Eswaraiah, V., Sankaranarayanan, V., & Ramaprabhu, S. (2011). Functionalized graphene–PVDF foam composites for EMI shielding. *Macromolecular Materials and Engineering*, 296(10), 894-898.
- Feng, H., Bai, D., Tan, L., Chen, N., & Wang, Y. (2017). Preparation and microwave-absorbing property of EP/BaFe₁₂O₁₉/PANI composites. *Journal of Magnetism and Magnetic Materials*, 433, 1-7.
- Gordani, G. R., Ghasemi, A., & Saidi, A. (2014). Enhanced magnetic properties of substituted Sr-hexaferrite nanoparticles synthesized by co-precipitation method. *Ceramics International*, 40(3), 4945-4952.
- Gairola, S. P., Verma, V., Singh, A., Purohit, L. P., & Kotnala, R. K. (2010). Modified composition of barium ferrite to act as a microwave absorber in X-band frequencies. *Solid State Communications*, 150(3-4), 147-151.
- Ghasemi, A., Hossienpour, A., Morisako, A., Saatchi, A., & Salehi, M. (2006). Electromagnetic properties and microwave absorbing characteristics of doped barium hexaferrite. *Journal of Magnetism and Magnetic Materials*, 302(2), 429-435.
- Ghasemi, A. (2011). Remarkable influence of carbon nanotubes on microwave absorption characteristics of strontium ferrite/CNT nanocomposites. *Journal of Magnetism and Magnetic Materials*, 323(23), 3133-3137.
- Ghasemi, A. (2013). The role of multi-walled carbon nanotubes on the magnetic and reflection loss characteristics of substituted strontium ferrite nanoparticles. *Journal of Magnetism and Magnetic Materials* 330, 163–168.
- Gordani, G. R., & Ghasemi, A. (2014). Optimization of carbon nanotube volume percentage for enhancement of high frequency magnetic properties of SrFe₈MgCoTi₂O₁₉/MWCNTs. *Journal of magnetism and magnetic materials*, 363, 49-54.
- Gultom, G., Rianna, M., Sebayang, P., & Ginting, M. (2020). The effect of Mg–Al binary doped barium hexaferrite for enhanced microwave absorption performance. *Case Studies in Thermal Engineering*, 18, 100580.
- Gunanto, Y. E., Izaak, M. P., Silaban, S. S., & Adi, W. A. (2018, May). Synthesis and Characterization of Barium-Hexaferrite-Based Nanocomposite on X-Band Microwave. In *IOP Conference Series: Materials Science and Engineering* (Vol. 367, No. 1, p. 012040). IOP Publishing.

- Goldman, A. (2006). *Modern ferrite technology*. Springer Science & Business Media.
- Gupta, M., & Leong, E. W. W. (2008). *Microwaves and metals*. John Wiley & Sons.
- Gunanto, Y. E., Jobiliong, E., & Adi, W. A. (2016). Microwave absorbing properties of $\text{Ba}_{0.6}\text{Sr}_{0.4}\text{Fe}_{12-z}\text{Mn}_z\text{O}_{19}$ ($z = 0-3$) materials in XBand frequencies. *Journal of Mathematical and Fundamental Sciences*, 48(1), 55-65.
- Gordani, G. R., Ghasemi, A., & Saidi, A. (2014). Enhanced magnetic properties of substituted Sr-hexaferrite nanoparticles synthesized by co-precipitation method. *Ceramics International*, 40(3), 4945-4952.
- Gul, I. H., Ahmed, W., & Maqsood, A. (2008). Electrical and magnetic characterization of nanocrystalline Ni–Zn ferrite synthesis by co-precipitation route. *Journal of Magnetism and Magnetic Materials*, 320(3-4), 270-275.
- Hajalilou, A., Hashim, M., Abbasi, M., Kamari, H. M., & Azimi, H. (2015). A comparative study on the effects of different milling atmospheres and sintering temperatures on the synthesis and magnetic behavior of spinel single phase $\text{Ni}_{0.64}\text{Zn}_{0.36}\text{Fe}_2\text{O}_4$ nanocrystals. *Journal of Materials Science: Materials in Electronics*, 26(10), 7468-7483.
- Haijun, Z., Zhichao, L., Xi, Y., Liangying, Z., & Mingzhong, W. (2003). Complex permittivity and permeability dependence of $\text{Ba}_4\text{Zn}_2\text{-ZCoZFe}_{36}\text{O}_{60}$ U-type hexaferrites prepared by citrate sol–gel on composition, annealing temperature and frequency. *Materials Science and Engineering: B*, 97(2), 160-166.
- Huang, L., Liu, X., & Yu, R. (2018). Enhanced microwave absorption properties of rod-shaped $\text{Fe}_2\text{O}_3/\text{Fe}_3\text{O}_4/\text{MWCNTs}$ composites. *Progress in Natural Science: Materials International*, 28(3), 288-295.
- Huang, X., Chen, J., Zhang, J., Wang, L., & Zhang, Q. (2010). A new microwave absorber based on antimony-doped tin oxide and ferrite composite with excellent electromagnetic match. *Journal of alloys and compounds*, 506(1), 347-350.
- Hu, S. L., Liu, J., Yu, H. Y., & Liu, Z. W. (2019). Synthesis and properties of barium ferrite nano-powders by chemical co-precipitation method. *Journal of Magnetism and Magnetic Materials*, 473, 79-84.
- Hirosawa, S., Hanaki, A., Tomizawa, H., & Hamamura, A. (1990). Current status of Nd-Fe-B permanent magnet materials. *Physica B: Condensed Matter*, 164(1-2), 117-123.

- Heck, I. C. (1974). *Magnetic Material and Its Applications*.
- Harris, V. G., Geiler, A., Chen, Y., Yoon, S. D., Wu, M., Yang, A., & Vittoria, C. (2009). Recent advances in processing and applications of microwave ferrites. *Journal of Magnetism and Magnetic Materials*, 321(14), 2035-2047.
- Handoko, E., Sugihartono, I., Budi, S., Randa, M., Jalil, Z., & Alaydrus, M. (2018, August). The effect of thickness on microwave absorbing properties of barium ferrite powder. In *Journal of Physics: Conference Series* (Vol. 1080, No. 1, p. 012002). IOP Publishing.
- Hai-Tao, L., Yang, L., Bin-Song, W., & Chen-Sha, L. (2015). Microwave Absorption Properties of Polyester Composites Incorporated with Heterostructure Nanofillers with Carbon Nanotubes as Carriers. *Chinese Physics Letters*, 32(4), 044102.
- Huo, J., Wang, L., & Yu, H. (2009). Polymeric nanocomposites for electromagnetic wave absorption. *Journal of materials science*, 44(15), 3917-3927.
- Haimbaugh, R. E. (2001). *Theory of heating by induction. Practical Induction Heat Treating*, 5-11.
- Iskander, M. F. 1992. *Electromagnetic Fields and Waves*. Englewood Cliffs, New Jersey: Prentice Hall.
- Idris, F. M., Hashim, M., Ismayadi, I., Idza, I. R., Manap, M., & Shafie, M. S. E. (2013). Broadening of EM energy-absorption frequency band by micrometer-to-nanometer grain size reduction in NiZn ferrite. *IEEE transactions on magnetics*, 49(11), 5475-5479.
- Idris, F. M., Hashim, M., Abbas, Z., Ismail, I., Nazlan, R., & Ibrahim, I. R. (2016). Recent developments of smart electromagnetic absorbers based polymer-composites at gigahertz frequencies. *Journal of Magnetism and Magnetic Materials*, 405, 197-208.
- Iqbal, M. J., Ashiq, M. N., & Gul, I. H. (2010). Physical, electrical and dielectric properties of Ca-substituted strontium hexaferrite (SrFe₁₂O₁₉) nanoparticles synthesized by co-precipitation method. *Journal of Magnetism and Magnetic Materials*, 322(13), 1720-1726.
- Ismail, I., Hashim, M., Matori, K. A., Alias, R., & Hassan, J. (2011). Milling time and BPR dependence on permeability and losses of Ni_{0.5}Zn_{0.5}Fe₂O₄ synthesized via mechanical alloying process. *Journal of magnetism and magnetic materials*, 323(11), 1470-1476.
- Jonscher, A. K. (1999). Dielectric relaxation in solids. *Journal of Physics D: Applied Physics*, 32(14), R57.

- Kools, F. X. N. M., & Stoppels, D. (1993). Kirk-Othmer Encyclopedia of Chem. Tech., Fourth Edition 10, 381-413.
- Kim, Y. J., & Kim, S. S. (2002). Microwave absorbing properties of Co-substituted Ni₂W hexaferrites in Ka-band frequencies (26.5-40 GHz). IEEE transactions on magnetics, 38(5), 3108-3110.
- Koops, C. G. (1951). On the dispersion of resistivity and dielectric constant of some semiconductors at audiofrequencies. Physical review, 83(1), 121.
- Kiani, E., Rozatian, A. S., & Yousefi, M. H. (2014). Structural, magnetic and microwave absorption properties of SrFe_{12-2x}(Mn_{0.5}Cd_{0.5}Zr)_xO₁₉ ferrite. Journal of magnetism and magnetic materials, 361, 25-29.
- Kreisel, J., Lucazeau, G., & Vincent, H. (1999). Raman study of substituted barium ferrite single crystals, BaFe_{12-2x}Me_xCoxO₁₉ (Me= Ir, Ti). Journal of Raman spectroscopy, 30(2), 115-120.
- Kreisel, J., Vincent, H., Tasset, F., Pate, M., & Ganne, J. P. (2001). An investigation of the magnetic anisotropy change in BaFe_{12-2x}TixCoxO₁₉ single crystals. Journal of Magnetism and Magnetic Materials, 224(1), 17-29.
- Koch, C. C. (1997). Synthesis of nanostructured materials by mechanical milling: problems and opportunities. Nanostructured Materials, 9(1-8), 13-22.
- Livingston, J. D. (1981). A review of coercivity mechanisms. Journal of Applied Physics, 52(3), 2544-2548.
- Li, G., Liu, M., Hao, C., Lei, Q., & Wei, Y. (2019). Conductivity and interface charge accumulation between XLPE and SIR for HVDC cable accessory. Journal of Materials Science: Materials in Electronics, 30(2), 1450-1457.
- Landau, L. D., Bell, J. S., Kearsley, M. J., Pitaevskii, L. P., Lifshitz, E. M., & Sykes, J. B. (2013). Electrodynamics of continuous media (Vol. 8). elsevier.
- Li, C. J., Wang, B., & Wang, J. N. (2012). Magnetic and microwave absorbing properties of electrospun Ba_(1-x)LaxFe₁₂O₁₉ nanofibers. Journal of Magnetism and Magnetic Materials, 324(7), 1305-1311.
- Lu, M., Li, H. L., & Lau, K. T. (2004). Formation and growth mechanism of dissimilar coiled carbon nanotubes by reduced-pressure catalytic chemical vapor deposition. The Journal of Physical Chemistry B, 108(20), 6186-6192.
- Limin, D., Zhidong, H. A. N., Zhang, Y., Ze, W. U., & Zhang, X. (2006). Synthesis

- of hexagonal barium ferrite nanoparticle by sol-gel method. *Rare Metals*, 25(6), 605-608.
- Lau, K. T., Lu, M., & Hui, D. (2006). Coiled carbon nanotubes: Synthesis and their potential applications in advanced composite structures. *Composites Part B: Engineering*, 37(6), 437-448.
- Lee, S. M. (2015). *International encyclopedia of composites*. VHC Publishers, New York 404-430.
- Li, J., Xu, T., Liu, L., Hong, Y., Song, Z., Bai, H., & Zhou, Z. (2021). Microstructure, magnetic and low-frequency microwave absorption properties of doped Co–Ti hexagonal barium ferrite nanoparticles. *Ceramics International*, 47(13), 19247-19253.
- Lagarkov, A. N., & Rozanov, K. N. (2009). High-frequency behavior of magnetic composites. *Journal of Magnetism and Magnetic Materials*, 321(14), 2082-2092.
- Li, Z., & Gao, F. (2011). Chemical bond and hardness of M, W-type hexagonal barium ferrites. *Canadian Journal of Chemistry*, 89(5), 573-576.
- Legodi, M. A., & De Waal, D. (2007). The preparation of magnetite, goethite, hematite and maghemite of pigment quality from mill scale iron waste. *Dyes and Pigments*. *Journal of Materials Science*, 74(1), 161-16.
- Liu, S., Luo, H., Yan, S., Yao, L., He, J., Li, Y., He, L., Huang, S., and Deng, L. (2017). Effect of Nd-doping on structure and microwave electromagnetic properties. *Journal of Magnetism and Magnetic Materials*, 426, 267–272. <https://doi.org/10.1016/j.jmmm.2016.11.080>.
- Matsumoto, M., Morisako, A., & Takei, S. (2001). Characteristics of Ba–ferrite thin films for magnetic disk media application. *Journal of alloys and compounds*, 326(1-2), 215-220.
- Meena, R. S., Bhattacharya, S., & Chatterjee, R. (2010). Complex permittivity, permeability and wide band microwave absorbing property of La³⁺ substituted U-type hexaferrite. *Journal of magnetism and magnetic materials*, 322(14), 1923-1928.
- Munir, A. (2017). Microwave radar absorbing properties of multiwalled carbon nanotubes polymer composites: a review. *Advances in Polymer Technology*, 36(3), 362-370.
- Meena, R. S., Bhattacharya, S., & Chatterjee, R. (2010). Complex permittivity, permeability and microwave absorbing properties of (Mn_{2-x}Zn_x) U-type hexaferrite. *Journal of Magnetism and Magnetic Materials*, 322(19), 2908-2914.

- Michielssen, E., Sajer, J. M., Ranjithan, S., & Mitra, R. (1993). Design of lightweight, broad-band microwave absorbers using genetic algorithms. *IEEE Transactions on Microwave Theory and Techniques*, 41(6), 1024-1031.
- Mustaffa, M. S., Abdullah, N. H., Ismail, I., & Ibrahim, I. R. (2019). An investigation of microstructural, magnetic and microwave absorption properties of multi-walled carbon nanotubes/ $\text{Ni}_{0.5}\text{Zn}_{0.5}\text{Fe}_2\text{O}_4$. *Scientific reports*, 9(1), 1-7.
- Mustaffa, M. S., & Shahrani, N. M. M. (2018). Sintering temperature effect on microstructure and magnetic evolution properties with nano-and micrometer grain size in ferrite polycrystals. In *Sintering Technology-Method and Application*. IntechOpen.
- Mehdizadeh, P., & Jahangiri, H. (2016). Effect of carbon black content on the microwave absorbing properties of CB/epoxy composites. *Journal of Nanostructures*, 6(2), 140-148.
- Moon, K. S., Choi, H. D., Lee, A. K., Cho, K. Y., Yoon, H. G., & Suh, K. S. (2000). Dielectric properties of epoxy-dielectrics-carbon black composite for phantom materials at radio frequencies. *Journal of applied polymer science*, 77(6), 1294-1302.
- Makeiff, D. A., & Huber, T. (2006). Microwave absorption by polyaniline-carbon nanotube composites. *Synthetic metals*, 156(7-8), 497-505.
- Maeda, T., Sugimoto, S., Kagotani, T., Tezuka, N., & Inomata, K. (2004). Effect of the soft/hard exchange interaction on natural resonance frequency and electromagnetic wave absorption of the rare earth-iron-boron compounds. *Journal of Magnetism and Magnetic Materials*, 281(2-3), 195-205.
- Mu, G., Pan, X., Chen, N., Gan, K., & Gu, M. (2008). Preparation and magnetic properties of barium hexaferrite nanorods. *Materials Research Bulletin*, 43(6), 1369-1375.
- Meng, P., Xiong, K., Ju, K., Li, S., & Xu, G. (2015). Wideband and enhanced microwave absorption performance of doped barium ferrite. *Journal of Magnetism and Magnetic Materials*, 385, 407-411.
- Meng, W., Yuping, D., Shunhua, L., Xiaogang, L., & Zhijiang, J. (2009). Absorption properties of carbonyl-iron/carbon black double-layer microwave absorbers. *Journal of Magnetism and Magnetic Materials*, 321(20), 3442-3446.
- Narang, S. B., Chawla, S. K., Mudsainiyan, R. K., & Pubby, K. (2015).

Comparative dielectric analysis of Co-Zr doped M-type barium hexaferrites $\text{BaCo}_x\text{Zr}_x\text{Fe}_{(12-2x)}\text{O}_{19}$ prepared by different wet chemical routes. *Integrated Ferroelectrics*, 167(1), 98-106.

Nadhirah, N., Muda, C., Azis, S., Hashim, M., Hassan, J., Sulaiman, S., Musa, M. A. (2015). Synthesis and Characterization of Barium Hexaferrites Derived from Steel Waste by Ammonium Nitrate Salt Melt Synthesis. *Journal Materials Science*, 16(1), 73–77.

Nikmanesh, H., Moradi, M., Bordbar, G. H., & Alam, R. S. (2016). Synthesis of multi-walled carbon nanotube/doped barium hexaferrite nanocomposites: An investigation of structural, magnetic and microwave absorption properties. *Ceramics International*, 42(13), 14342-14349.

Nikmanesh, H., Hoghoghifard, S., & Hadi-Sichani, B. (2019). Study of the structural, magnetic, and microwave absorption properties of the simultaneous substitution of several cations in the barium hexaferrite structure. *Journal of Alloys and Compounds*, 775, 1101-1108.

Narang, S. B., & Pubby, K. (2016). Single-layer & double-layer microwave absorbers based on Co–Ti substituted barium hexaferrites for application in X and Ku-band. *Journal of Materials Research*, 31(23), 3682-3693.

Nakamura, T. (2000). Snoek's limit in high-frequency permeability of polycrystalline Ni–Zn, Mg–Zn, and Ni–Zn–Cu spinel ferrites. *Journal of applied physics*, 88(1), 348-353.

Pereira, F. M. M., Santos, M. R. P., Sohn, R. S. T. M., Almeida, J. S., Medeiros, A. M. L., Costa, M. M., & Sombra, A. S. B. (2009). Magnetic and dielectric properties of the M-type barium strontium hexaferrite ($\text{Ba}_x\text{Sr}_{1-x}\text{Fe}_{12}\text{O}_{19}$) in the RF and microwave (MW) frequency range. *Journal of Materials Science: Materials in Electronics*, 20(5), 408-417.

Pullar, R. C. (2012). Hexagonal ferrites: a review of the synthesis, properties and applications of hexaferrite ceramics. *Progress in Materials Science*, 57(7), 1191-1334.

Peng, J. P., Zhang, H., Tang, L. C., Jia, Y., & Zhang, Z. (2013). Dielectric properties of carbon nanotubes/epoxy composites. *Journal of nanoscience and nanotechnology*, 13(2), 964-969.

Pullar, R. C. (2014). Multiferroic and magnetoelectric hexagonal ferrites. In *Mesoscopic Phenomena in Multifunctional Materials* (pp. 159-200). Springer, Berlin, Heidelberg.

Phan, C. H., Mariatti, M., & Koh, Y. H. (2016). Electromagnetic interference

shielding performance of epoxy composites filled with multiwalled carbon nanotubes/manganese zinc ferrite hybrid fillers. *Journal of Magnetism and Magnetic Materials*, 401, 472-478.

Qiu, J., Shen, H., & Gu, M. (2005). Microwave absorption of nanosized barium ferrite particles prepared using high-energy ball milling. *Powder Technology*, 154(2-3), 116-119.

Qin, F., & Brosseau, C. (2012). A review and analysis of microwave absorption in polymer composites filled with carbonaceous particles. *Journal of applied physics*, 111(6), 4.

Rodziah, N., Hashim, M., Idza, I. R., Ismayadi, I., Hapishah, A. N., and Khamirul, M. A. (2012). Dependence of developing magnetic hysteresis characteristics on stages of evolving microstructure in polycrystalline yttrium iron garnet. *Applied Surface Science*, 258(7), 2679–2685. <https://doi.org/10.1016/j.apsusc.2011.10.117>

Rezlescu, L., Rezlescu, E., Popa, P. D., & Rezlescu, N. (1999). Fine barium hexaferrite powder prepared by the crystallisation of glass. *Journal of Magnetism and Magnetic Materials*, 193(1-3), 288-290

Rodriguez, N. M., Chambers, A., & Baker, R. T. K. (1995). Catalytic engineering of carbon nanostructures. *Langmuir*, 11(10), 3862-3866.

Rosdi, N., Mustafa, M. S., Abdullah, N. H., Sulaiman, S., & Ling, T. T. (2019). Synthesis and characterization of Mg–Ti substituted barium hexaferrite ($\text{BaMg}_{0.6}\text{Ti}_{0.6}\text{Fe}_{10.8}\text{O}_{19}$) derived from millscale waste for microwave application. *Journal of Materials Science: Materials in Electronics*, 30(9), 8636-8644.

Rehman, A. U., Abbas, S. M., Ammad, H. M., Badshah, A., Ali, Z., & Anjum, D. H. (2013). A facile and novel approach towards carboxylic acid functionalization of multiwalled carbon nanotubes and efficient water dispersion. *Materials Letters*, 108, 253-256.

Rosdi, N., Azis, R. A. S., Ismail, I., Mokhtar, N., Muhammad Zulkimi, M. M., & Mustafa, M. S. (2021). Structural, microstructural, magnetic and electromagnetic absorption properties of spiraled multiwalled carbon nanotubes/barium hexaferrite (MWCNTs/ $\text{BaFe}_{12}\text{O}_{19}$) hybrid. *Scientific Reports*, 11(1), 1-14.

Rosdi, N., Azis, R. A. S., Ismail, I., Mustafa, M. S & Mokhtar, N (2019). Effect of Sintering Temperatures on Structural, Magnetic and Microwave Properties of Barium Ferrites/Epoxy Composites. *International Journal of Innovative Technology and Exploring Engineering (IJITEE)*, 9(1), 2278-3075.

Rana, K., Thakur, P., Tomar, M., Gupta, V., & Thakur, A. (2018). Investigation

of cobalt substituted M-type barium ferrite synthesized via co-precipitation method for radar absorbing material in Ku-band (12–18 GHz). *Ceramics International*, 44(6), 6370-6375.

Rianna, M., Situmorang, M., Kurniawan, C., Tetuko, A. P., Setiadi, E. A., Ginting, M., & Sebayang, P. (2019). The effect of Mg-Al additive composition on microstructure, magnetic properties, and microwave absorption on $\text{BaFe}_{12-2x}\text{Mg}_x\text{Al}_x\text{O}_{19}$ ($x= 0-0.5$) material synthesized from natural iron sand. *Materials Letters*, 256, 126612.

Ruan, S., Xu, B., Suo, H., Wu, F., Xiang, S., & Zhao, M. (2000). Microwave absorptive behavior of ZnCo-substituted W-type Ba hexaferrite nanocrystalline composite material. *Journal of Magnetism and Magnetic Materials*, 212(1-2), 175-177.

Risman, P. (1991). Terminology and notation of microwave power and electromagnetic energy. *Journal of microwave power and Electromagnetic energy*, 26(4), 243-250.

Ramo, S., Whinnery, J. R., & Whinnery, J. A. (1944). *Fields and waves in modern radio*. J. Wiley and Sons, Incorporated.

Stiegler, J. O., & Mansur, L. K. (1979). Radiation effects in structural materials. *Annual review of materials science*, 9(1), 405-454.

Stefan, I., Chiriac, R., Nicoara, V., Cioatera, N., Nicolicescu, C., Trotea, M., & Ghercioiu, J. (2011). PM Functional Materials: Research Regarding Structural Transformations of M Type Barium Ferrite Piro-synthesis. In *European Congress and Exhibition on Powder Metallurgy*. European PM Conference Proceedings (p. 1). The European Powder Metallurgy Association.

Sugimoto, S., Kondo, S., Okayama, K., Nakamura, H., Book, D., Kagotani, T., & Sato, R. (1999). M-type ferrite composite as a microwave absorber with wide bandwidth in the GHz range. *IEEE Transactions on Magnetics*, 35(5), 3154-3156.

Singhal, S., Namgyal, T., Singh, J., Chandra, K., & Bansal, S. (2011). A comparative study on the magnetic properties of $\text{MFe}_{12}\text{O}_{19}$ and $\text{MAlFe}_{11}\text{O}_{19}$ (M= Sr, Ba and Pb) hexaferrites with different morphologies. *Ceramics International*, 37(6), 1833-1837.

Syazwan, M. M., Hashim, M., Azis, R. S., Ismail, I., Kanagesan, S., & Hapishah, A. N. (2017). Enhancing absorption properties of Mg–Ti substituted barium hexaferrite nanocomposite through the addition of MWCNT. *Journal of Materials Science: Materials in Electronics*, 28(12), 8429-8436.

Shaikjee, A., & Coville, N. J. (2012). *The synthesis, properties and uses of*

- carbon materials with helical morphology. *Journal of Advanced Research*, 3(3), 195-223.
- Shukla, V. (2019). Review of electromagnetic interference shielding materials fabricated by iron ingredients. *Nanoscale Advances*, 1(5), 1640-1671.
- Shi, D., Cheng, J. P., Liu, F., & Zhang, X. B. (2010). Controlling the size and size distribution of magnetite nanoparticles on carbon nanotubes. *Journal of Alloys and Compounds*, 502(2), 365-370
- Smit, J., & Wijn, H. P. J. (1959). *Ferrites*, Philips technical library. Eindhoven, The Netherlands, 278.
- Sugimoto M. In: Wohfarth EP, editor. *Ferromagnetic materials*, vol. 3. Amsterdam: North-Holland Physics Publishing; 1980. p. 392–440.
- Sözeri, H., Deligöz, H., Kavas, H., & Baykal, A. (2014). Magnetic, dielectric and microwave properties of M–Ti substituted barium hexaferrites (M= Mn²⁺, Co²⁺, Cu²⁺, Ni²⁺, Zn²⁺). *Ceramics International*, 40(6), 8645-8657.
- Sai, R., Shivashankar, S. A., Yamaguchi, M., & Bhat, N. (2017). Magnetic nanoferrites for RF CMOS: Enabling 5G and beyond. *The Electrochemical Society Interface*, 26(4), 71.
- Sulaiman, N. I., Bakar, M. A., Bakar, N. H. H. A., & Hussin, M. H. (2019, April). Sol-gel synthesis of barium hexaferrite and their catalytic application in methyl ester synthesis. In *IOP Conference Series: Materials Science and Engineering* (Vol. 509, No. 1, p. 012103). IOP Publishing.
- Snoek, J. L. (1946). *Non Metallic Magnetic Material for High Frequencies*.
- Smit, J., & Wijn, H. P. J. (1959). *Ferrites*, Philips technical library. Eindhoven, The Netherlands, 278.
- Saville, P. (2005). *Review of radar absorbing materials*. Defence Research and Development Atlantic Dartmouth (Canada).
- Sun, J., Wang, W., & Yue, Q. (2016). Review on microwave-matter interaction fundamentals and efficient microwave-associated heating strategies. *Materials*, 9(4), 231.
- Tong, X. C. (2016). *Advanced materials and design for electromagnetic interference shielding*. CRC press.
- Tyagi, S., Baskey, H. B., Agarwala, R. C., Agarwala, V., & Shami, T. C. (2011). Development of hard/soft ferrite nanocomposite for enhanced microwave absorption. *Ceramics International*, 37(7), 2631-2641.
- Topal, U., Ozkan, H., & Dorosinskii, L. (2007). Finding optimal Fe/Ba ratio to

- obtain single phase BaFe₁₂O₁₉ prepared by ammonium nitrate melt technique. *Journal of alloys and compounds*, 428(1-2), 17-21.
- Topal, U., & Bakan, H. I. (2010). Permanently magnetic BaFe₁₂O₁₉ foams: Synthesis and characterization. *Materials Chemistry and Physics*, 123(1), 121-124.
- Tang, X., & Hu, K. A. (2007). Preparation and electromagnetic wave absorption properties of Fe-doped zinc oxide coated barium ferrite composites. *Materials Science and Engineering: B*, 139(2-3), 119-123.
- Tan, L., Liu, Q., Jing, X., Liu, J., Song, D., Hu, S., & Wang, J. (2015). Removal of uranium (VI) ions from aqueous solution by magnetic cobalt ferrite/multiwalled carbon nanotubes composites. *Chemical Engineering Journal*, 273, 307-315.
- Valenzuela, R. (2012). Novel applications of ferrites. *Physics Research International*, 2012.
- Vinnik, D. A., Zhivulin, V. E., Trofimov, E. A., Starikov, A. Y., Zherebtsov, D. A., Zaitseva, O. V., & Trukhanov, A. V. (2019). Extremely polysubstituted magnetic material based on magnetoplumbite with a hexagonal structure: synthesis, structure, properties, prospects. *Nanomaterials*, 9(4), 559.
- Vinoy, K. J., & Jha, R. M. (1996). Radar absorbing materials- From theory to design and characterization(Book). Boston, MA: Kluwer Academic Publishers, 1996.
- Von Aulock, W. H., Boxer, A. S., Ollom, J. F., & Rauchmiller, R. F. (1965). *Handbook of Microwave Ferrite Materials*. Edited by Wilhelm H. Von Aulock. Contributors: Arnold S. Boher, John F. Ollom, Robert F. Rauchmiller. Academic Press.
- Veisi, S. S., Yousefi, M., Amini, M. M., Shakeri, A. R., & Bagherzadeh, M. (2019). Magnetic and microwave absorption properties of Cu/Zr doped M-type Ba/Sr hexaferrites prepared via sol-gel auto-combustion method. *Journal of Alloys and Compounds*, 773, 1187-1194.
- Verma, A., Goel, T. C., & Mendiratta, R. G. (2000). Frequency variation of initial permeability of NiZn ferrites prepared by the citrate precursor method. *Journal of Magnetism and Magnetic Materials*, 210(1-3), 274-278.
- Wang, L., Song, J., Zhang, Q., Huang, X., & Xu, N. (2009). The microwave magnetic performance of Sm³⁺ doped BaCo₂Fe₁₆O₂₇. *Journal of Alloys and Compounds*, 481(1-2), 863-866.
- Wang, J., Zhou, H., Zhuang, J., & Liu, Q. (2015). Magnetic γ -Fe₂O₃, Fe₃O₄, and

Fe nanoparticles confined within ordered mesoporous carbons as efficient microwave absorbers. *Physical Chemistry Chemical Physics*, 17(5), 3802-3812.

- Wang, T., Liu, Z., Lu, M., Wen, B., Ouyang, Q., Chen, Y., & Qi, L. (2013). Graphene-Fe₃O₄ nanohybrids: synthesis and excellent electromagnetic absorption properties. *Journal of Applied Physics*, 113(2), 024314.
- Wadhawan, A., Garrett, D., & Pérez, J. M. (2003). Nanoparticle-assisted microwave absorption by single-wall carbon nanotubes. *Applied Physics Letters*, 83(13), 2683-2685.
- Wen, F., Yi, H., Qiao, L., Zheng, H., Zhou, D., & Li, F. (2008). Analyses on double resonance behavior in microwave magnetic permeability of multiwalled carbon nanotube composites containing Ni catalyst. *Applied physics letters*, 92(4), 042507.
- Wu, M., Zhang, Y. D., Hui, S., Xiao, T. D., Ge, S., Hines, W. A., & Taylor, G. W. (2002). Microwave magnetic properties of Co₅₀/(SiO₂)₅₀ nanoparticles. *Applied Physics Letters*, 80(23), 4404-4406.
- Wu, Z. P., Li, M. M., Hu, Y. Y., Li, Y. S., Wang, Z. X., Yin, Y. H., & Zhou, X. (2011). Electromagnetic interference shielding of carbon nanotube macrofilms. *Scripta Materialia*, 64(9), 809-812.
- Wang, Y., Huang, Y., & Ding, J. (2014). Synthesis and electromagnetic absorption properties of polypyrrole/BaFe₁₂O₁₉-Ni_{0.8}Zn_{0.2}Fe₂O₄/multiwalled carbon nanotube composites. *Materials science in semiconductor processing*, 26, 632-641.
- Wang, Q., Zhou, F., Ding, X., Zhou, Z., Wang, C., Zhang, W., & Lee, S. T. (2013). Microstructure and water-lubricated friction and wear properties of CrN (C) coatings with different carbon contents. *Applied Surface Science*, 268, 579-587.
- Xiong, Y., Luo, H., Nie, Y., Chen, F., Dai, W., Wang, X., & Gong, R. (2019). Synergistic effect of silica coated porous rodlike nickel ferrite and multiwalled carbon nanotube with improved electromagnetic wave absorption performance. *Journal of Alloys and Compounds*, 802, 364-372.
- Xie, J., Han, M., Chen, L., Kuang, R., & Deng, L. (2007). Microwave-absorbing properties of NiCoZn spinel ferrites. *Journal of magnetism and magnetic materials*, 314(1), 37-42.
- Yuzcelik, C. K. (2003). Radar absorbing material design.
- Yang, Y., Zhang, B., Xu, W., Shi, Y., Zhou, N., & Lu, H. (2003). Microwave

absorption studies of W-hexaferrite prepared by coprecipitation/mechanical milling. *Journal of magnetism and magnetic materials*, 265(2), 119-122.

Yue, Y., Han, P., Dong, S., Zhang, K., Zhang, C., Shang, C., & Cui, G. (2012). Nanostructured transition metal nitride composites as energy storage material. *Chinese Science Bulletin*, 57(32), 4111-4118.

Yang, Y., Xu, C., Xia, Y., Wang, T., & Li, F. (2010). Synthesis and microwave absorption properties of FeCo nanoplates. *Journal of Alloys and Compounds*, 493(1-2), 549-552.

Yan, J., Huang, Y., Chen, C., Liu, X., & Liu, H. (2019). The 3D CoNi alloy particles embedded in N-doped porous carbon foams for high-performance microwave absorbers. *Carbon*, 152, 545-555.

Zhang, Z., Liu, X., Wang, X., Wu, Y., & Li, R. (2012). Effect of Nd-Co substitution on magnetic and microwave absorption properties of SrFe₁₂O₁₉ hexaferrites. *Journal of Alloys and Compounds*, 525, 114-119.

Zhao, P. Y., Wang, H. Y., & Wang, G. S. (2020). Enhanced electromagnetic absorption properties of commercial Ni/MWCNTs composites by adjusting dielectric properties. *Frontiers in Chemistry*, 8, 97.

Zhao, B., Deng, J., Liang, L., Zuo, C., Bai, Z., Guo, X., & Zhang, R. (2017). Lightweight porous Co₃O₄ and Co/CoO nanofibers with tunable impedance match and configuration-dependent microwave absorption properties. *CrystEngComm*, 19(41), 6095-6106.

Zhao, B., Liang, L., Deng, J., Bai, Z., Liu, J., Guo, X., & Zhang, R. (2017). 1D Cu@Ni nanorods anchored on 2D reduced graphene oxide with interfacial engineering to enhance microwave absorption properties. *CrystEngComm*, 19(44), 6579-6587.

Zhuravlev, V. A., Minin, R. M., Itin, V. I., Lopushnyak, Y. M., Zhuravlev, A. V., & Lilenko, E. P. (2017). Study of the magnetic anisotropy of the multiphase samples of the ferrimagnets with hexagonal crystal structure by the method of ferromagnetic resonance. In *IOP Conference Series: Materials Science and Engineering* (Vol. 168, No. 1, p. 012081). IOP Publishing.

Zhang, Q., Li, C., Chen, Y., Han, Z., Wang, H., Wang, Z., & Zhang, Z. (2010). Effect of metal grain size on multiple microwave resonances of Fe/TiO₂ metal-semiconductor composite. *Applied Physics Letters*, 97(13), 133115.

Zhu, H. Y., Jiang, R., Huang, S. H., Yao, J., Fu, F. Q., & Li, J. B. (2015). Novel

magnetic NiFe_2O_4 /multi-walled carbon nanotubes hybrids: facile synthesis, characterization, and application to the treatment of dyeing wastewater. *Ceramics International*, 41(9), 11625-11631.

Zhang, Y., & Zhai, Y. (2011). Magnetic induction heating of nano-sized ferrite particle. In *advances in induction and microwave heating of mineral and organic materials*. IntechOpen.

Zeng, X., Cheng, X., Yu, R., & Stucky, G. D. (2020). Electromagnetic microwave absorption theory and recent achievements in microwave absorbers. *Carbon*.

